1
Ion Sources

In the ion sources, the analysed samples are ionized prior to analysis in the mass spectrometer. A variety of ionization techniques are used for mass spectrometry. The most important considerations are the internal energy transferred during the ionization process and the physico-chemical properties of the analyte that can be ionized. Some ionization techniques are very energetic and cause extensive fragmentation. Other techniques are softer and only produce ions of the molecular species. Electron ionization, chemical ionization and field ionization are only suitable for gas-phase ionization and thus their use is limited to compounds sufficiently volatile and thermally stable. However, a large number of compounds are thermally labile or do not have sufficient vapour pressure. Molecules of these compounds must be directly extracted from the condensed to the gas phase.

These direct ion sources exist under two types: liquid-phase ion sources and solid-state ion sources. In liquid-phase ion sources the analyte is in solution. This solution is introduced, by nebulization, as droplets into the source where ions are produced at atmospheric pressure and focused into the mass spectrometer through some vacuum pumping stages. Electrospray, atmospheric pressure chemical ionization and atmospheric pressure photoionization sources correspond to this type. In solid-state ion sources, the analyte is in an involatile deposit. It is obtained by various preparation methods which frequently involve the introduction of a matrix that can be either a solid or a viscous fluid. This deposit is then irradiated by energetic particles or photons that desorb ions near the surface of the deposit. These ions can be extracted by an electric field and focused towards the analyser. Matrix-assisted laser desorption, secondary ion mass spectrometry, plasma desorption and field desorption sources all use this strategy to produce ions. Fast atom bombardment uses an involatile liquid matrix.

The ion sources produce ions mainly by ionizing a neutral molecule in the gas phase through electron ejection, electron capture, protonation, deprotonation, adduct formation or by the transfer of a charged species from a condensed phase to the gas phase. Ion production often implies gas-phase ion–molecule reactions. A brief description of such reactions is given at the end of the chapter.

1.1 Electron Ionization

The electron ionization (EI) source, formerly called electron impact, was devised by Dempster and improved by Bleakney [1] and Nier [2]. It is widely used in organic mass spectrometry. This ionization technique works well for many gas-phase molecules but induces extensive fragmentation so that the molecular ions are not always observed.

As shown in Figure 1.1, this source consists of a heated filament giving off electrons. The latter are accelerated towards an anode and collide with the gaseous molecules of
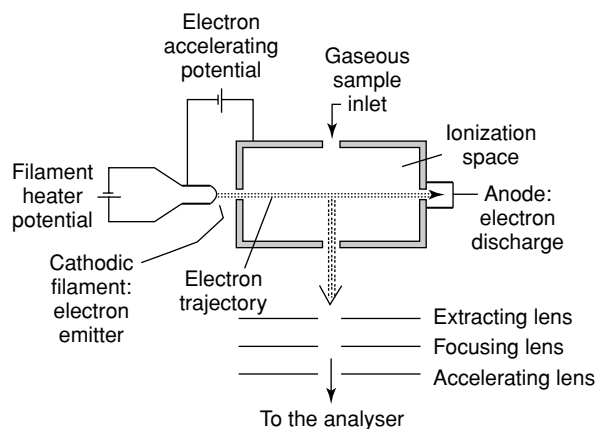
Figure 1.1
Diagram of an electron ionization source.

the analysed sample injected into the source. Gases and samples with high vapour pressure are introduced directly into the source. Liquids and solids are usually heated to increase the vapour pressure for analysis.

Each electron is associated to a wave whose wavelength λ is given by

$$\lambda = \frac{h}{mv}$$

where m is its mass, v its velocity and h Planck's constant. This wavelength is 2.7 Å for a kinetic energy of 20 eV and 1.4 Å for 70 eV. When this wavelength is close to the bond lengths, the wave is disturbed and becomes complex. If one of the frequencies has an energy hv corresponding to a transition in the molecule, an energy transfer that leads to various electronic excitations can occur [3]. When there is enough energy, an electron can be expelled. The electrons do not 'impact' molecules. For this reason, it is recommended that the term electron impact must be avoided.

Figure 1.2 displays a typical curve of the number of ions produced by a given electron current, at constant pressure of the sample, when the acceleration potential of the electrons (or their kinetic energy) is varied [4]. At low potentials the energy is lower than the molecule ionization energy. At high potentials, the wavelength becomes very small and molecules become 'transparent' to these electrons. In the case of organic molecules, a wide maximum appears around 70 eV. At this level, small changes in the electron energy do not significantly affect the pattern of the spectrum.

On average, one ion is produced for every 1000 molecules entering the source under the usual spectrometer conditions, at 70 eV. Furthermore, between 10 and 20 eV is transferred to the molecules during the ionization process. Since approximately 10 eV is enough to ionize most organic molecules, the excess energy leads to extensive fragmentation. This fragmentation can be useful because it provides structural information for the elucidation of unknown analytes.

At a given acceleration potential and at constant temperature, the number of ions I produced per unit time in a volume V is linked to the pressure p and to the electron current
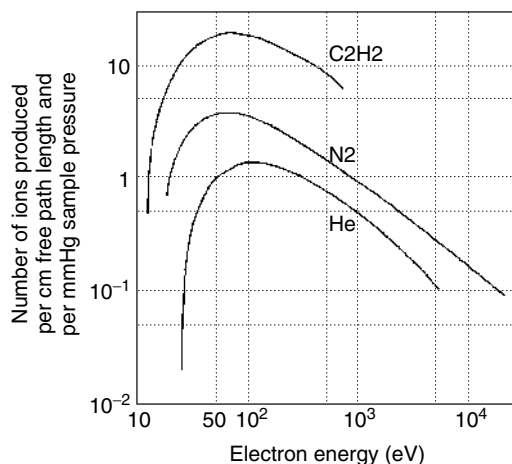
Figure 1.2
Number of ions produced as a function of the
electron energy. A wide maximum appears around
70 eV.

i through the following equation, where N is a constant proportionality coefficient:

$$I = N p i V$$

This equation shows that the sample pressure is directly correlated with the resulting ionic current. This allows such a source to be used in quantitative measurements.

Figure 1.3 displays two EI spectra of the same β-lactam compound, obtained at 70 and 15 eV. Obviously, at lower energy there is less fragmentation. At first glance, the molecular ion is better detected at low energy. However, the absolute intensity, in arbitrary units, proportional to the number of detected ions, is actually lower: about 250 units at 70 eV and 150 units at 15 eV. Thus, the increase in relative intensity, due to the lower fragmentation, is illusory. Actually, there is a general loss of intensity due to the decrease in ionization efficiency at lower electron energy. This will generally be the rule, so that the method is not very useful for better detection of the molecular ion. However, the lowering of the ionization voltage may favour some fragmentation processes.

A modification implies desorbing the sample from a heated rhenium filament near the electronic beam. This method is called desorption electron ionization (DEI).

Under conventional electron ionization conditions, the formation of negative ions is inefficient compared with the formation of positive ions.

1.2 Chemical Ionization

Electron ionization leads to fragmentation of the molecular ion, which sometimes prevents its detection. Chemical ionization (CI) is a technique that produces ions with little excess energy. Thus this technique presents the advantage of yielding a spectrum with less fragmentation in which the molecular species is easily recognized. Consequently, chemical ionization is complementary to electron ionization.
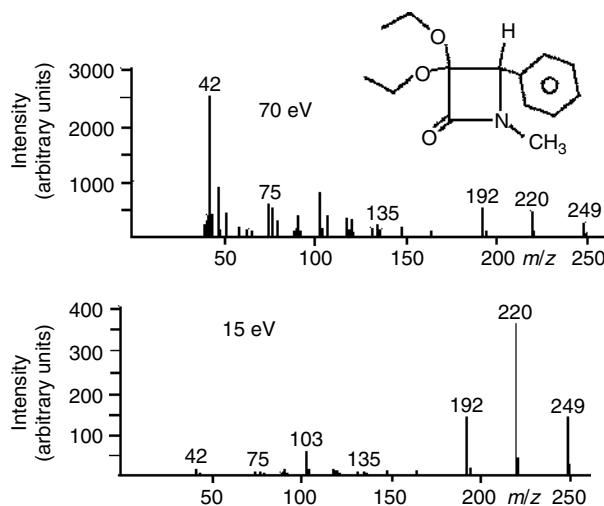
Figure 1.3
Two spectra of β-lactam. While the relative intensity of the
molecular ion peak is greater at lower ionization energy,
its absolute intensity, as read from the left-hand scale, is
actually somewhat reduced.

Chemical ionization [5] consists of producing ions through a collision of the molecule
to be analysed with primary ions present in the source. Ion–molecule collisions will thus
be induced in a definite part of the source. In order to do so, the local pressure has to
be sufficient to allow for frequent collisions. We saw that the mean free path could be
calculated from Equation 1 (see the Introduction). At a pressure of approximately 60 Pa,
the free path is about 0.1 mm. The source is then devised so as to maintain a local pressure
of that magnitude. A solution consists of introducing into the source a small box about 1 cm
along its side as is shown in Figure 1.4.

Two lateral holes allow for the crossing of electrons and another hole at the bottom
allows the product ions to pass through. Moreover, there is a reagent gas input tube and an
opening for the sample intake. The sample is introduced by means of a probe which will
close the opening.

This probe carries the sample within a hollow or contains the end part of a capillary
coming from a chromatograph or carries a filament on which the sample was deposited.
In the last case, we talk about desorption chemical ionization (DCI). The pumping speed
is sufficient to maintain a 60 Pa pressure within the box. Outside, the usual pressure in a
source, about 10^{-3} Pa, will be maintained.

Inside the box, the sample pressure will amount to a small fraction of the reagent
gas pressure. Thus, an electron entering the box will preferentially ionize the reagent gas
molecules through electron ionization. The resulting ion will then mostly collide with other
reagent gas molecules, thus creating an ionization plasma through a series of reactions. Both
positive and negative ions of the substance to be analysed will be formed by chemical reac-
tions with ions in this plasma. This causes proton transfer reactions, hydride abstractions,
adduct formations, charge transfers, and so on.

This plasma will also contain low-energy electrons, called thermal electrons. These are
either electrons that were used for the first ionization and later slowed, or electrons produced
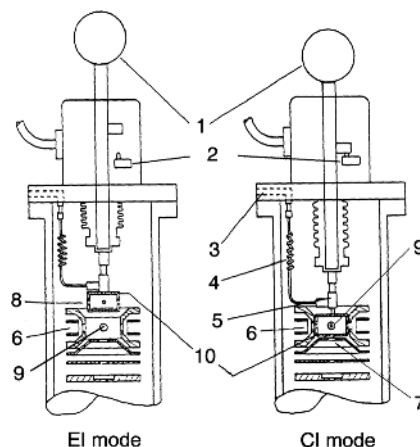
Figure 1.4
Combined EI and CI source. Lowering
the box 10 switches from the EI to CI
mode. (1) EI/CI switch; in EI mode, the
box serves as a pusher; (2) microswitch;
(3) entrance for the reagent gas; (4) flex-
ible capillary carrying the reagent gas;
(5) diaphragm; (6) filament giving off
electrons; (7) path of the ions towards
the analyser inlet; (8) hole for the ion-
izing electrons in CI mode; (9) sample in-
let; (10) box with holes, also named 'ion
volume'. From Finnigan MAT 44S docu-
mentation. Reprinted, with permission.

by ionization reactions. These slow electrons may be associated with molecules, thereby
yielding negative ions by electron capture.

   Ions produced from a molecule by the abstraction of a proton or a hydride, or the
addition of a proton or of another ion, are termed ions of the molecular species or, less
often, pseudomolecular ions. They allow the determination of the molecular mass of the
molecules in the sample. The term molecular ions refers to $M^{\bullet +}$ or $M^{\bullet -}$ ions.

1.2.1 Proton Transfer

Among the wide variety of possible ionization reactions, the most common is proton trans-
fer. Indeed, when analyte molecules M are introduced in the ionization plasma, the reagent
gas ions GH^+ can often transfer a proton to the molecules M and produce protonated
molecular ions MH^+. This chemical ionization reaction can be described as an acid–base
reaction, the reagent gas ions GH^+ and the analyte molecules being Brönsted acid (pro-
ton donor) and Brönsted base (proton acceptor) respectively. The tendency for a reagent
ion GH^+ to protonate a particular analyte molecule M may be assessed from its proton
affinity values. The proton affinity (PA) is the negative enthalpy change for the protonation
reaction (see Appendix 6). The observation of protonated molecular ions MH^+ implies
that the analyte molecule M has a proton affinity much higher than that of the reagent gas
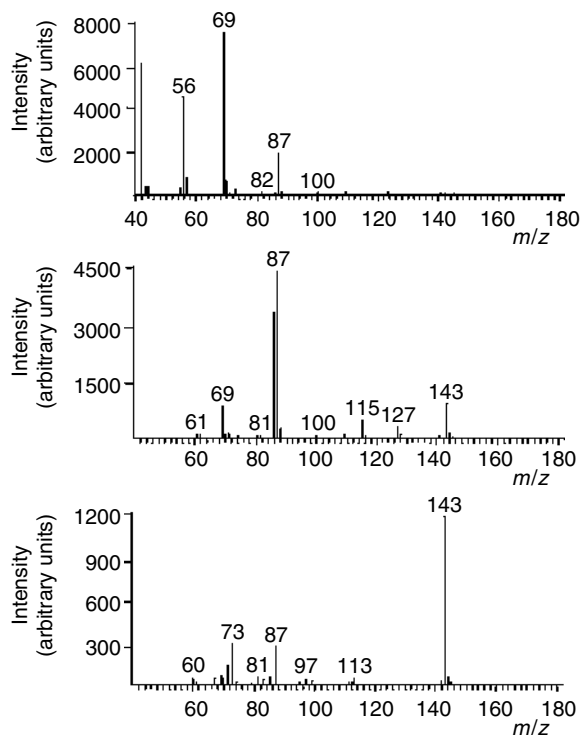
Figure 1.5
EI (top), methane CI (middle) and isobutane CI (bottom)
mass spectra of butyl methacrylate. The ionization tech-
niques (EI vs CI) and the reagent gases (methane vs isobu-
tane) influence the amount of fragmentation and the
prominence of the protonated molecular ions detected
at 143 Th.

(PA(M) > PA(G)). If the reagent gas has a proton affinity much higher than that of an analyte
(PA(G) > PA(M)), proton transfer from GH^+ to M will be energetically too unfavourable.

The selectivity in the types of compound that can be protonated and the internal energy
of the resulting protonated molecular ion depends on the relative proton affinities of
the reagent gas and the analyte. From the thermalizing collisions, this energy depends
also on the ion source temperature and pressure. The energetics of the proton transfer
can be controlled by using different reagent gases. The most common reagent gases are
methane (PA = 5.7 eV), isobutane (PA = 8.5 eV) and ammonia (PA = 9.0 eV). Not only are
isobutane and ammonia more selective, but protonation of a compound by these reagent
gases is considerably less exothermic than protonation by methane. Thus, fragmentation
may occur with methane while with isobutane or ammonia the spectrum often presents
solely a protonated molecular ion.

The differences between EI and CI spectra are clearly illustrated in Figure 1.5. Indeed,
the EI spectrum of butyl methacrylate displays a very low molecular ion at *m/z* 142. In
contrast, its CI spectra exhibit the protonated molecular ion at *m/z* 143, and very few

fragmentations. This example shows also the control of the fragmentation degree in CI by changing the reagent gas. Methane and isobutane CI mass spectra of butyl methacrylate give the protonated molecular ions, but the degree of fragmentation is different. With isobutane, the base peak is the protonated molecular ion at m/z 143, whereas with methane the base peak is a fragment ion at m/z 87.

1.2.2 Adduct Formation

In CI plasma, all the ions are liable to associate with polar molecules to form adducts, a kind of gas-phase solvation. The process is favoured by the possible formation of hydrogen bonds. For the adduct to be stable, the excess energy must be eliminated, a process which requires a collision with a third partner. The reaction rate equation observed in the formation of these adducts is indeed third order. Ions resulting from the association of a reagent gas molecule G with a protonated molecular ion MH^+ or with a fragment ion F^+, of a protonated molecular ion MH^+ with a neutral molecule, and so on, are often found in CI spectra. Every ion in the plasma may become associated with either a sample molecule or a reagent gas molecule. Some of these ions are useful in the confirmation of the molecular mass, such as

$$MH^+ + M \longrightarrow (2M + H)^+$$

$$F^+ + M \longrightarrow (F + M)^+$$
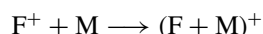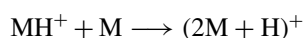
These associations are often useful to identify a mixture or to determine the molecular masses of the constituents of the mixture. In fact, a mixture of two species M and N can give rise to associations such as $(MH + N)^+$, $(F + N)^+$ with $(F + M)^+$, and so on. Adducts resulting from neutral species obtained by neutralization of fragments, or by a neutral loss during a fragmentation, are always at much too low concentrations to be observed.

It is always useful to examine the peaks appearing beyond the ions of the molecular species of a substance thought to be pure. If some peaks cannot be explained by reasonable associations, a mixture must be suspected.

Figure 1.6 shows an example of CI spectra for a pure sample and for a mixture. When interpreting the results, one must always keep in mind that a mixture that is observed may result from the presence of several constituents before the vaporization or from their formation after the vaporization.

The first spectrum contains the peaks of various adducts of the molecular ion of a pure compound. The second spectrum is that of a substance that is initially pure, as shown by other analysis, but appears as a mixture in the gas phase as it loses either hydrogen cyanide or water.

1.2.3 Charge-Transfer Chemical Ionization

Rare gases, nitrogen, carbon monoxide and other gases with high ionization potential react by charge exchange:

$$Xe + e^- \longrightarrow Xe^{\bullet+} + 2e^-$$

$$Xe^{\bullet+} + M \longrightarrow M^{\bullet+} + Xe$$

A radical cation is obtained, as in EI, but with a smaller energy content. Less fragmentation is thus observed. In practice, these gases are not used very often.
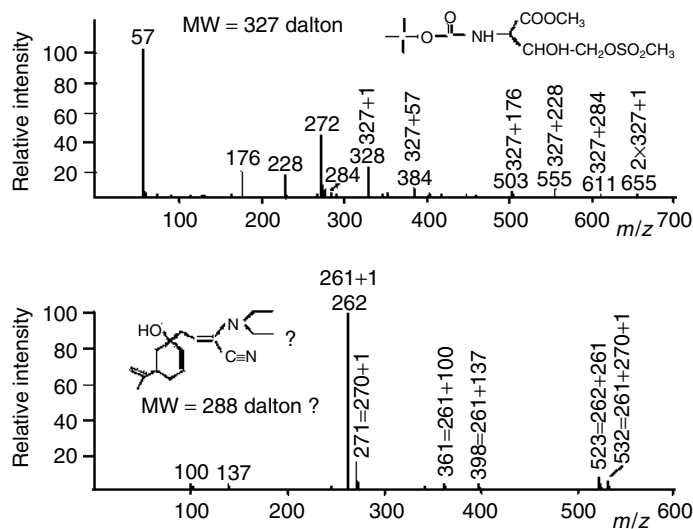
Figure 1.6
Two examples of chemical ionization (isobutane) spectra. The top
spectrum is that of a pure compound. The bottom spectrum is that
of a mixture of two compounds with masses 261 and 270. They
correspond respectively to the loss of hydrogen cyanide and water.

1.2.4 Reagent Gas

1.2.4.1 Methane as Reagent Gas

If methane is introduced into the ion volume through the tube, the primary reaction with
the electrons will be a classical EI reaction:

$$CH_4 + e^- \longrightarrow CH_4^{\bullet+} + 2e^-$$
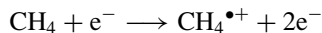
This ion will fragment, mainly through the following reactions:

$$CH_4^{\bullet+} \longrightarrow CH_3^+ + H^\bullet$$
$$CH_4^{\bullet+} \longrightarrow CH_2^{\bullet+} + H_2$$
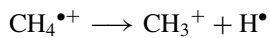
However, mostly, it will collide and react with other methane molecules yielding

$$CH_4^{\bullet+} + CH_4 \longrightarrow CH_5^+ + CH_3^\bullet$$

Other ion–molecule reactions with methane will occur in the plasma, such as

$$CH_3^+ + CH_4 \longrightarrow C_2H_5^+ + H_2$$
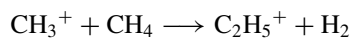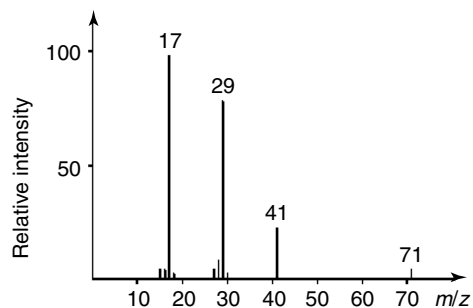
Figure 1.7
Spectrum of methane ionization plasma at
20 Pa. The relative intensities depend on the
pressure in the source.

A $C_3H_5^+$ ion is formed by the following successive reactions:

$$CH_2^{\bullet +} + CH_4 \longrightarrow C_2H_3^+ + H_2 + H^\bullet$$

$$C_2H_3^+ + CH_4 \longrightarrow C_3H_5^+ + H_2$$
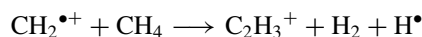
The relative abundance of all these ions will depend on the pressure. Figure 1.7 shows the
spectrum of the plasma obtained at 200 μbar (20 Pa). Taking CH_5^+, the most abundant ion,
as a reference (100 %), $C_2H_5^+$ amounts to 83 % and $C_3H_5^+$ to 14 %.

Unless it is a saturated hydrocarbon, the sample will mostly react by acquiring a proton
in an acid–base type of reaction with one of the plasma ions, for example

$$M + CH_5^+ \longrightarrow MH^+ + CH_4$$
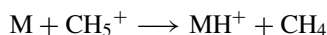
A systematic study showed that the main ionizing reactions of molecules containing het-
eroatoms occurred through acid–base reactions with $C_2H_5^+$ and $C_3H_5^+$. If, however, the
sample is a saturated hydrocarbon RH, the ionization reaction will be a hydride abstraction:

$$RH + CH_5^+ \longrightarrow R^+ + CH_4 + H_2$$
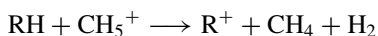
Moreover, ion–molecule adduct formation is observed in the case of polar molecules, a
type of gas-phase solvation, for example

$$M + CH_3^+ \longrightarrow (M + CH_3)^+$$

The ions $(MH)^+$, R^+ and $(M + CH_3)^+$ and other adducts of ions with the molecule are
termed molecular species or, less often, pseudomolecular ions. They allow the determination
of the molecular mass of the molecules in the sample.

1.2.4.2 Isobutane as Reagent Gas

Isobutane loses an electron upon EI and yields the corresponding radical cation, which will
fragment mainly through the loss of a hydrogen radical to yield a *t*-butyl cation, and to a
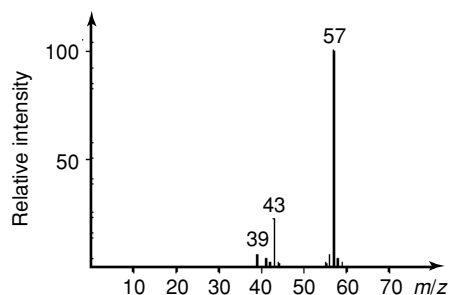
Figure 1.8
Spectrum of the isobutane plasma under chemical ionization conditions at 200 μbar.

lesser extent through the loss of a methyl radical:
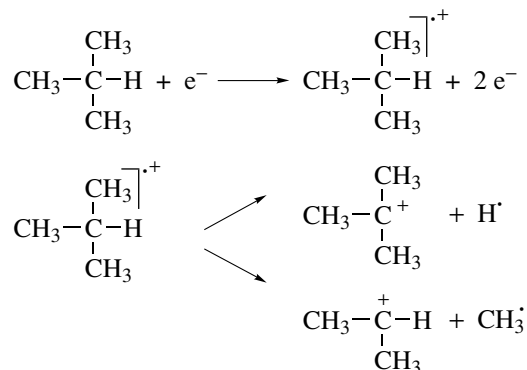
An ion with mass 39 Da is also observed in its spectrum (Figure 1.8) which corresponds to $C_3H_3^+$. Neither its formation mechanism nor its structure are known, but it is possible that it is the aromatic cyclopropenium ion.

Here again, the plasma ions will mainly react through proton transfer to the sample, but polar molecules will also form adducts with the *t*-butyl ions $(M + 57)^+$ and with $C_3H_3^+$, yielding $(M + 39)^+$ among others.

This isobutane plasma will be very inefficient in ionizing hydrocarbons because the *t*-butyl cation is relatively stable. This characteristic allows its use in order to detect specifically various substances in mixtures containing also hydrocarbons.

1.2.4.3 Ammonia as Reagent Gas

The radical cation generated by EI reacts with an ammonia molecule to yield the ammonium ion and the $NH_2^\bullet$ radical:

$$NH_3^{\bullet+} + NH_3 \longrightarrow NH_4^+ + NH_2^\bullet$$
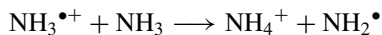
An ion with mass 35 Da is observed in the plasma (Figure 1.9) which results from the association of an ammonium ion and an ammonia molecule:

$$NH_4^+ + NH_3 \longrightarrow (NH_4 + NH_3)^+$$
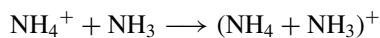
This adduct represents 15 % of the intensity of the ammonium ion at 200 μbar.
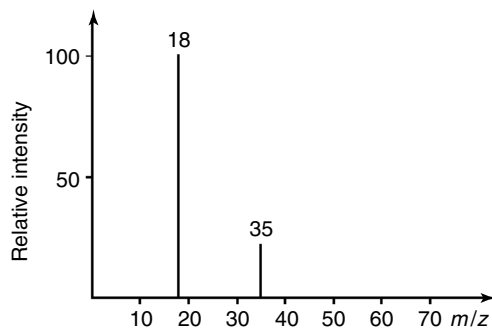
Figure 1.9
Spectrum of an ammonia ionization plasma at
$200\,\mu$bar.

In this gas, the ionization mode will depend on the nature of the sample. The basic molecules, mostly amines, will ionize through a proton transfer:

$$RNH_2 + NH_4^+ \longrightarrow RNH_3^+ + NH_3$$
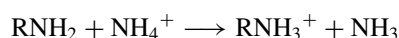
Polar molecules and those able to form hydrogen bonds while presenting no or little basic character will form adducts. In intermediate cases, two pseudomolecular ions $(M + 1)^+$ and $(M + 18)^+$ will be observed. Compounds that do not correspond to the criteria listed above, for example saturated hydrocarbons, will not be efficiently ionized. Alkanes, aromatics, ethers and nitrogen compounds other than amines will not be greatly ionized. Comparing spectra measured with various reagent gases will thus be very instructive. For example, the detection, in the presence of a wealth of saturated hydrocarbons, of a few compounds liable to be ionized is possible, as shown in Figure 1.10.

1.2.5 Negative Ion Formation

Almost all neutral substances are able to yield positive ions, whereas negative ions require the presence of acidic groups or electronegative elements to produce them. This allows some selectivity for their detection in mixtures. Negative ions can be produced by capture of thermal electrons by the analyte molecule or by ion–molecule reactions between analyte and ions present in the reagent plasma.

All CI plasmas contain electrons with low energies, issued either directly from the filament but deactivated through collisions, or mostly from primary ionization reactions, which produce two low-energy electrons through the ionization reaction. The interaction of electrons with molecules leads to negative ion production by three different mechanisms [5]:

$$AB + e^- \longrightarrow AB^{\bullet -} \quad \text{(associative resonance capture)}$$

$$AB + e^- \longrightarrow A^\bullet + B^- \quad \text{(dissociative resonance capture)}$$

$$AB + e^- \longrightarrow A^+ + B^- + e^- \quad \text{(ion pair production)}$$
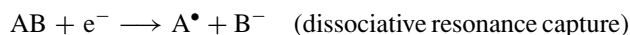
These electrons can be captured by a molecule. The process can be associative or dissociative. The associative resonance capture that leads to the formation of negative molecular
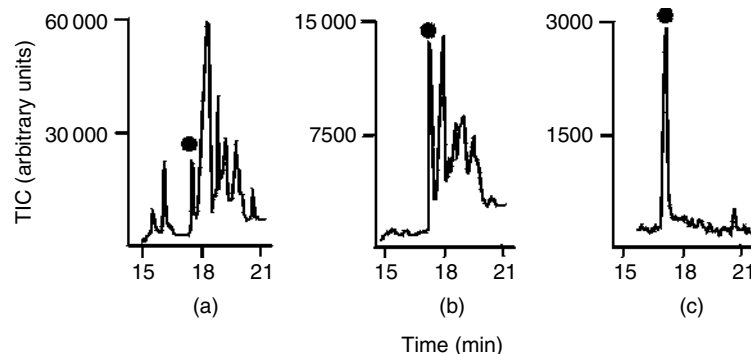
Figure 1.10
GC/MS TIC traces of butyl methacrylate dissolved in C11–C12 saturated
hydrocarbon. (a) EI. The peak corresponding to butyl methacrylate is
marked by a dot. The peaks following are C11 saturated hydrocarbons.
(b) Same trace obtained by CI usig methane as reagent gas. Butyl methacry-
late (dot) is still well detected, but the trace of the hydrocarbons is aten-
uated. (c) CI using isobutane as reagent gas. Butyl methacrylate is well
detected, while the hydrocarbons are almost not detected.

ions needs electrons in the energy range 0–2 eV, whereas the dissociative resonance capture
is observed with electrons of 0–15 eV and leads to the formation of negative fragment
ions.

The associative resonance capture is favoured for molecules with several electroneg-
ative atoms or with possibilities to stabilize ions by resonance. The energy to remove
an electron from the molecular anion by autodetachment is generally very low. Conse-
quently, any excess of energy from the negative molecular ion as it is formed must be
removed by collision. Thus, in CI conditions, the reagent gas serves not only for producing
thermal electrons but also as a source of molecules for collisions to stabilize the formed
ions.

Ion pair production is observed with a wide range of electron energies above 15 eV.
It is principally this process that leads to negative ion production under conventional EI
conditions. Ion pair production forms structurally insignificant very low-mass ions with a
sensitivity that is 3–4 orders of magnitude lower than that for positive ion production.

The need to detect tetrachlorodioxins with high sensitivity has contributed to the devel-
opment of negative ion CI. In some cases, the detection sensitivity with electron capture is
better than with positive ions. It can be explained by the high mobility of the electron that
ensures a greater rate of electron attachment than the rate of ion formation involving transfer
of a much larger particle. However, electron capture is very dependent on the experimental
conditions and thus can be irreproducible.

Note the different behaviours that the electron can adopt towards the molecules. Elec-
trons at thermal equilibrium, that is those whose kinetic energy is less than about 1 eV
($1\,eV = 98\,kJ\,mol^{-1}$), can be captured by molecules and yield negative radical anions.
Those whose energy lies between 1 and a few hundred electronvolts behave as a wave and
transfer energy to molecules, without any 'collisions'. Finally, molecules will be 'transpar-
ent' to the electrons with higher energies: here we enter the field of electron microscopy.

As already discussed, negative ions can also be formed through ion–molecule reactions with one of the plasma ions. These reactions can be an acid–base reaction or an addition reaction through adduct formation.

The mixture, CH_4–N_2O 75:25, is very useful because of the following reactions involving low-energy electrons:

$$N_2O + e^- \longrightarrow N_2O^{\bullet -}$$

$$N_2O^{\bullet -} \longrightarrow N_2 + O^{\bullet -}$$

$$O^{\bullet -} + CH_4 \longrightarrow CH_3^{\bullet} + OH^-$$
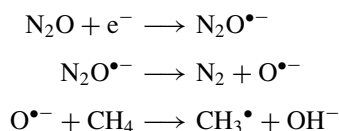
This plasma also contains other ions. The advantage derives from the simultaneous presence of thermal electrons, allowing the capture of electrons, and of a basic ion, OH^-, which reacts with acidic compounds in the most classical acid–base reaction. Because of the presence of the methane, the same mixture is also suitable for positive ion production.

The energy balance for the formation of negative ions appears as in the following example (PhOH = phenol) [6]:

$$
\begin{array}{ll}
H^+ + OH^- \longrightarrow H_2O & \Delta H^\circ = -1634.7 \text{ kJ mol}^{-1} \\
PhOh \longrightarrow PhO^- + H^+ & \Delta H^\circ = +145 \text{ kJ mol}^{-1} \\
\hline
PhOH + OH^- \longrightarrow PhO^- + H_2O & \Delta H^\circ = -178.7 \text{ kJ mol}^{-1}
\end{array}
$$
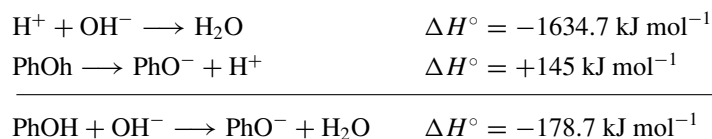
The exothermicity of the reaction is the result of the formation of H_2O, which is neutral and carries off the excess energy. The product anion will be 'cold'.

However, during a positive ionization, the following will occur:

$$
\begin{array}{ll}
CH_5^+ \longrightarrow CH_4 + H^+ & \Delta H^\circ = +543.5 \text{ kJ mol}^{-1} \\
(C_2H_5)_2S + H^+ \longrightarrow (C_2H_5)_2SH^+ & \Delta H^\circ = -856.7 \text{ kJ mol}^{-1} \\
\hline
CH_5^+ + (C_2H_5)_2S \longrightarrow (C_2H_5)_2SH^+ + CH_4 & \Delta H^\circ = -313.2 \text{ kJ mol}^{-1}
\end{array}
$$
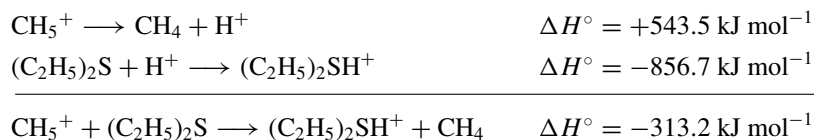
In this case, the exothermicity comes mainly from the association of the proton with the molecule to be ionized. The resulting cation will contain an appreciable level of excess energy.

1.2.6 Desorption Chemical Ionization

Baldwin and McLafferty [7] noticed that introducing a sample directly into the CI plasma on a glass or a metal support allowed the temperature for the observation of the mass spectrum to be reduced, sometimes by as much as $150\,^\circ C$. This prevents the pyrolysis of non-volatile samples. A drop of the sample in solution is applied on a rhenium or tungsten wire. The solvent is then evaporated and the probe introduced into the mass spectrometer source. The sample is desorbed by rapidly heating the filament by passing a controllable electric current through the wire. The ion formation from these compounds sometimes last for only a very short time, and the ions of the molecular species are observed for only a few seconds. The spectrum appearance generally varies with the temperature. Figure 1.11 displays the spectrum of mannitol obtained by the desorption chemical ionization (DCI) technique.
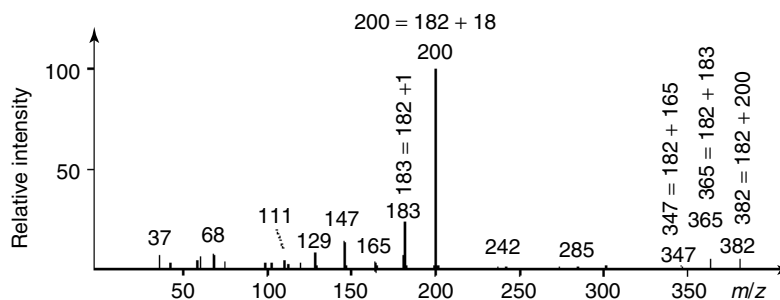
Figure 1.11
DCI spectrum of mannitol, a non-volatile compound, with H_2O as an reagent
gas. Note that water yields radical cation adducts $(M + H_2O)^{\bullet+}$.

The observed spectrum probably results from the superposition of several phenomena: evaporation of the sample with rapid ionization, direct ionization on the surface of the filament, direct ion desorption and, at higher temperature, pyrolysis followed by ionization.

Generally, the molecular species ion is clearly detected in the case of non-volatile compounds. The method can be useful, for example, for tetrasaccharides, small peptides, nucleic acids and other organic salts, which can be detected in either the positive or negative ion mode.

1.3 Field Ionization

Field ionization (FI) is a method that uses very strong electric fields to produce ions from gas-phase molecules. Its use as a soft ionization method in organic mass spectrometry is principally due to Beckey [8]. Like EI or CI, FI is only suitable for gas-phase ionization. Therefore, the sample is introduced into the FI source by the same techniques that are commonly used in EI and CI sources, for example using a direct probe that can be heated or the eluent from a gas chromatograph.

The intense electric fields used in this ionization method are generally produced by a potential difference of 8–12 kV that is applied between a filament called the emitter and a counter-electrode that is a few millimetres distant. Sample molecules in the gas phase approach the surface of the emitter that is held at high positive potential. If the electric field at the surface is sufficiently intense, that is if its strength reaches about 10^7–10^8 V cm^{-1}, one of the electrons from the sample molecule is transferred to the emitter by quantum tunnelling, resulting in the formation of a radical cation $M^{\bullet+}$. This ion is repelled by the emitter and flies towards the negative counter-electrode. A hole in the counter-electrode allows the ion to pass into the mass analyser compartment. In order to achieve the high electric field necessary for ionization, the emitter constituted of tungsten or rhenium filament is covered with thousands of carbon microneedles on its surface. It is at the tips of these microneedles that the electric field strength reaches its maximum. FI leads to the formation of $M^{\bullet+}$ and/or MH^+ ions depending on the analyte. The formation of protonated molecular species results from ion–molecule reactions that can occur between the initial ion and the sample molecules close to the surface of the emitter. It is not unusual to observe both $M^{\bullet+}$ and MH^+ in the FI spectrum.
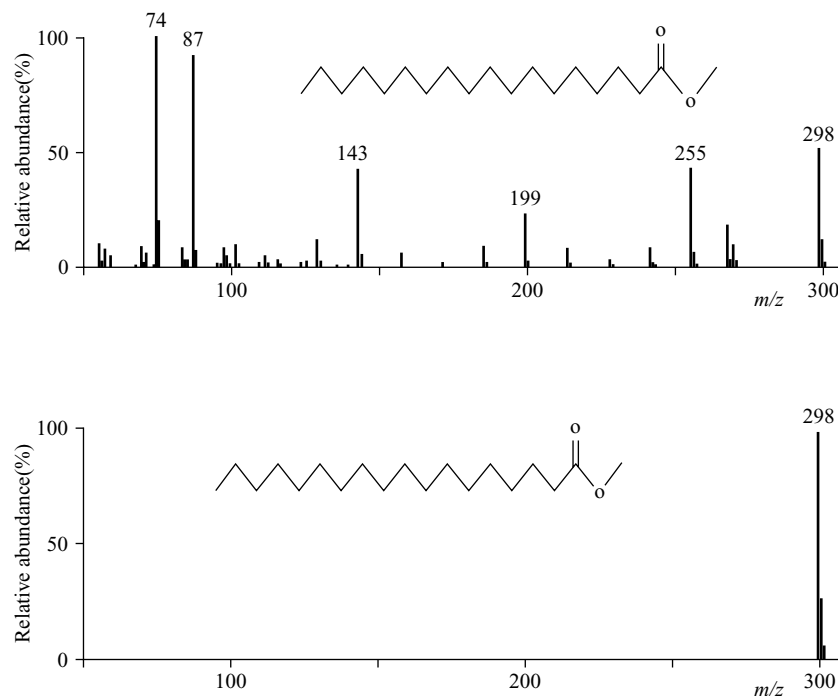
Figure 1.12
Comparison of EI (top) and FI (bottom) spectra of methyl stearate. Field ionization
yields simple spectrum that shows intense molecular ion detected at *m/z* 298 with-
out fragmentation. Reproduced, with permission from Micromass documentation.

The energy transferred in the FI process corresponds to a fraction of 1 electronvolt. So,
this ionization source generates ions with an extremely low excess of internal energy thus
exhibiting no fragmentation, as shown in Figure 1.12. As the internal energy of the ions
is much lower than that resulting in EI and CI processes, FI is one of the softest methods
to produce ions from organic molecules. However, thermal decomposition of the analyte
can occur during its evaporation prior to ionization. Therefore, FI allows molecular species
to be easily recognized only for compounds sufficiently volatile and thermally stable. For
instance, FI has proven to be a method of choice for the analysis of highly complex mixtures
such as fossil fuels. Generally, FI is complementary to EI and CI. It is used when EI and CI
fail to give ions of the molecular species, although it is not as sensitive. Indeed, this process
has very low ionization efficiency.

1.4 Fast Atom Bombardment and Liquid Secondary Ion Mass Spectrometry

Secondary ion mass spectrometry (SIMS) analyses the secondary ions emitted when a
surface is irradiated with an energetic primary ion beam [9, 10]. Ion sources with very
low-current primary ion beams are called static sources because they do not damage the

surface of the sample, as opposed to dynamic sources that produce surface erosion. Static SIMS causes less damage to any molecules on the surface than dynamic SIMS and gives spectra that can be similar to those obtained by plasma desorption [11]. This technique is mostly used with solids and is especially useful to study conducting surfaces. High-resolution chemical maps are produced by scanning a tightly focused ionizing beam across the surface.

Fast atom bombardment (FAB) [12] and liquid secondary ion mass spectrometry (LSIMS) [13] are techniques that consist of focusing on the sample a high primary current beam of neutral atoms/molecules or ions, respectively. Essential features of these two ionization techniques are that the sample must be dissolved in a non-volatile liquid matrix. In practice, glycerol is most often used, while *m*-nitrobenzylic alcohol (MNBA) is a good liquid matrix for non-polar compounds, and di- and triethanolamine are efficient, owing to their basicity, in producing negative ions. Thioglycerol and a eutectic mixture of dithiothreitol and dithioerythritol (5:1 w/w), referred to as magic bullet, are alternatives to glycerol.

These techniques use current beams that are in dynamic SIMS high enough to damage the surface. But they produce ions from the surface, as in static SIMS, because convection and diffusion inside the matrix continuously create a fresh layer from the surface for producing new ions. The energetic particles hit the sample solution, inducing a shock wave which ejects ions and molecules from the solution. Ions are accelerated by a potential difference towards the analyser. These techniques induce little or no ionization. They generally eject into the gas phase ions that were already present in the solution.

Under these conditions, both ion and neutral bombardment are practical techniques. The neutral atom beam at about 5 keV is obtained by ionizing a compound, most often argon, sometimes xenon. Ions are accelerated and focused towards the compound to be analysed under several kilovolts. They then go through a collision cell where they are neutralized by charge exchange between atoms and ions. Their momentum is sufficient to maintain the focusing. The remaining ions are then eliminated from the beam as it passes between electrodes. A diagram of such a source is shown in Figure 1.13. The reaction may be written as follows:

$$Ar^{\bullet+}{}_{(rapid)} + Ar_{(slow)} \longrightarrow Ar^{\bullet+}{}_{(slow)} + Ar_{(rapid)}$$
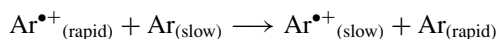
Using a 'caesium gun', one produces a beam of Cs^+ ions at about 30 keV. It is claimed to give better sensitivity than a neutral atom beam for high molecular weights. However, the advantage of using neutral molecules instead of ions lies in the avoidance of an accumulation of charges in the non-conducting samples.

This method is very efficient for producing ions from polar compounds with high molecular weights. Ions up to 10 000 Da and above can be observed, such as peptides and nucleotides. Moreover, it often produces ion beams that can be maintained during long periods of time, sometimes several tens of minutes, which allows several types of analysis to be carried out. This advantage is especially appreciated in measurements using multiple analysers (MS/MS). Other desorption techniques, such as DCI or field desorption (FD) (see later), generally give rise to transient signals, lasting only a few seconds at most. However, FAB or LSIMS requires a matrix such as glycerol, whose ions make the spectrum more complex. DCI and FD do not impose this inconvenience.
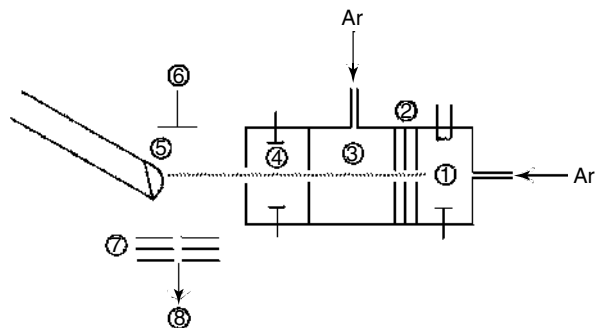
Figure 1.13
Diagram of an FAB gun. 1, Ionization of argon; the re-
sulting ions are accelerated and focused by the lenses 2.
In 3, the argon ions exchange their charge with neutral
atoms, thus becoming rapid neutral atoms. As the beam
path passes between the electrodes 4, all ionic species are
deflected. Only rapid neutral atoms reach the sample dis-
solved in a drop of glycerol, 5. The ions ejected from the
drop are accelerated by the pusher, 6, and focused by the
electrodes, 7, towards the analyser, 8.

Figure 1.14 displays an example of FABMS and MS/MS applied to the detection of
peptides in a mixture and the sequence determination of one of them.

1.5 Field Desorption

The introduction of field desorption (FD) as a method for the analysis of non-volatile
molecules is principally due to Beckey [14].

Based on FI, already described, FD has been developed as the first method that combines
desorption and ionization of the analyte. There is no need for evaporation of the analyte prior
to ionization. Consequently, FD is particularly suitable for analysing high-molecular-mass
and/or thermally labile compounds.

In FD, the sample is deposited, through evaporation of a solution also containing a
salt, on a tungsten or rhenium filament covered with carbon microneedles. A potential
difference is set between this filament and an electrode so as to obtain a field that can
go up to 10^8 V cm^{-1}. The filament is heated until the sample melts. The ions migrate
and accumulate at the tip of the needles, where they end up being desorbed, carrying along
molecules of the sample. Ionization occurs in the condensed phase or near the surface of the
filament by interaction with the high electric field according to the same mechanism as FI.
FD produces ions of extremely low internal energy thus exhibiting almost no fragmentation
and an abundant molecular species.

The technique is demanding and requires an experienced operator. It has now been
largely replaced by other desorption techniques. However, it remains an excellent method
to ionize high-molecular-mass non-polar compounds such as polymers.
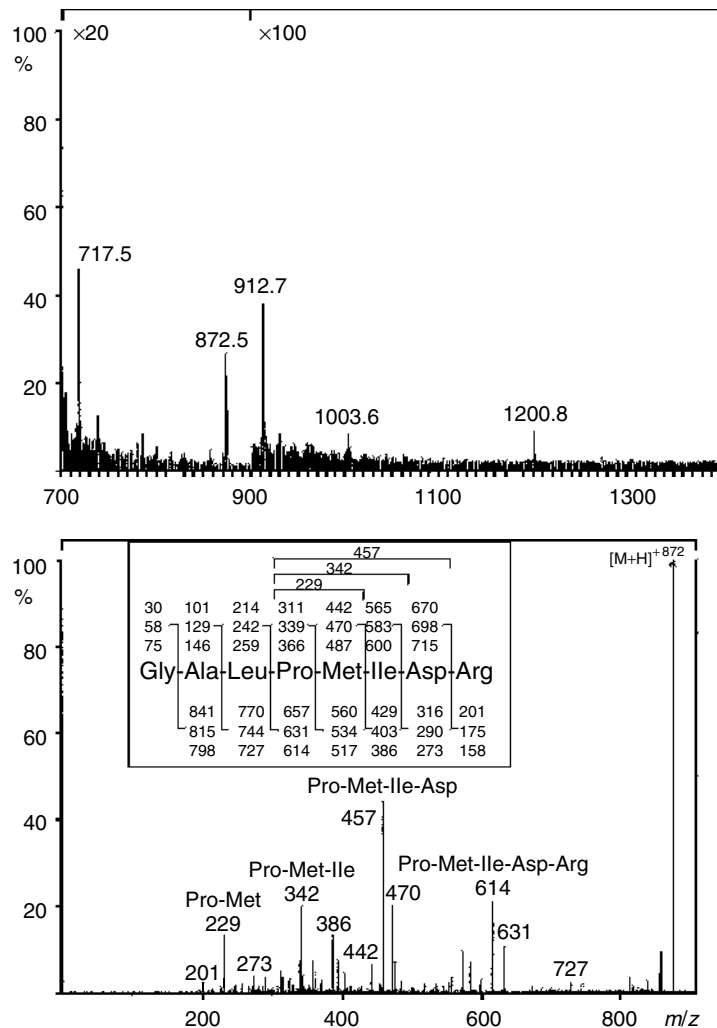
Figure 1.14
Top: FAB mass spectrum of a mixture of five peptides. The m/z of the protonated molecular ion $(M + H)^+$ of each of them is observed. Bottom: product ion tandem mass spectrum of the $(M + H)^+$ ion with m/z 872, giving the sequence of this peptide alone. The values within the frame are the masses of the various possible fragments for the indicated sequence.

1.6 Plasma Desorption

Plasma desorption (PD) was introduced by Mcfarlane and Torgesson [15]. In this ionization technique, the sample deposited on a small aluminized nylon foil is exposed in the source to the fission fragments of ^{252}Cf, having an energy of several mega-electronvolts.

The shock waves resulting from a bombardment of a few thousand fragments per second induce the desorption of neutrals and ions. This technique has allowed the observation of ions above 10 000 Da [16]. However, nowadays it is of limited use and has been replaced mainly by matrix-assisted laser desorption ionization.

1.7 Laser Desorption

Laser desorption (LD) is an efficient method for producing gaseous ions. Generally, laser pulses yielding from 10^6 to 10^{10} W cm^{-2} are focused on a sample surface of about 10^{-3}–10^{-4} cm^2, most often a solid. These laser pulses ablate material from the surface, and create a microplasma of ions and neutral molecules which may react among themselves in the dense vapour phase near the sample surface. The laser pulse realizes both the vaporization and the ionization of the sample.

This technique is used in the study of surfaces and in the analysis of the local composition of samples, such as inclusions in minerals or in cell organelles. It normally allows selective ionization by adjusting the laser wavelength. However, in most conventional infrared LD modes, the laser creates a thermal spike, and thus it is not necessary to match the laser wavelength with the sample.

Since the signals are very short, simultaneous detection analysers or time-of-flight analysers are required. The probability of obtaining a useful mass spectrum depends critically on the specific physical proprieties of the analyte (e.g. photoabsorption, volatility, etc.). Furthermore, the produced ions are almost always fragmentation products of the original molecule if its mass is above approximately 500 Da. This situation changed dramatically with the development of matrix-assisted laser desorption ionization (MALDI) [17, 18].

1.8 Matrix-Assisted Laser Desorption Ionization

This was introduced in 1988 principally by Karas and Hillenkamp [19–21]. It has since become a widespread and powerful source for the production of intact gas-phase ions from a broad range of large, non-volatile and thermally labile compounds such as proteins, oligonucleotides, synthetic polymers and large inorganic compounds. The use of a MALDI matrix, which provides for both desorption and ionization, is the crucial factor for the success of this ionization method. The method is characterized by easy sample preparation and has a large tolerance to contaminantion by salts, buffers, detergents, and so on [22, 23].

1.8.1 Principles of MALDI

MALDI is achieved in two steps. In the first step, the compound to be analysed is dissolved in a solvent containing in solution small organic molecules, called the matrix. These molecules must have a strong absorption at the laser wavelength. This mixture is dried before analysis and any liquid solvent used in the preparation of the solution is removed. The result is a 'solid solution' deposit of analyte-doped matrix crystals. The analyte molecules are embedded throughout the matrix so that they are completely isolated from one another.

The second step occurs under vacuum conditions inside the source of the mass spectrometer. This step involves ablation of bulk portions of this solid solution by intense laser
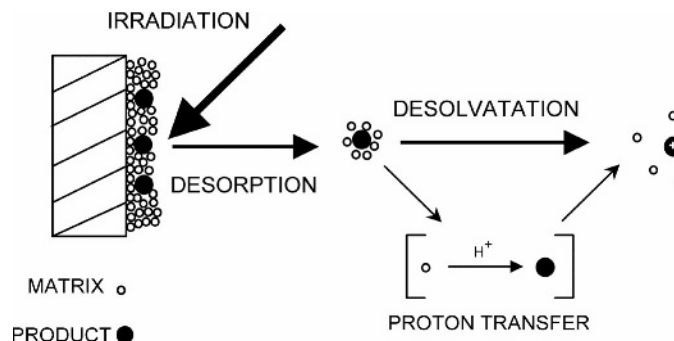
Figure 1.15
Diagram of the principle of MALDI.

pulses over a short duration. The exact mechanism of the MALDI process is not completely elucidated [24,25]. However, irradiation by the laser induces rapid heating of the crystals by the accumulation of a large amount of energy in the condensed phase through excitation of the matrix molecules. The rapid heating causes localized sublimation of the matrix crystals, ablation of a portion of the crystal surface and expansion of the matrix into the gas phase, entraining intact analyte in the expanding matrix plume [26].

Ionization reactions can occur under vacuum conditions at any time during this process but the origin of ions produced in MALDI is still not fully understood [27,28]. Among the chemical and physical ionization pathways suggested for MALDI are gas-phase photoionization, excited state proton transfer, ion–molecule reactions, desorption of preformed ions, and so on. The most widely accepted ion formation mechanism involves proton transfer in the solid phase before desorption or gas-phase proton transfer in the expanding plume from photoionized matrix molecules. The ions in the gas phase are then accelerated by an electrostatic field towards the analyser. Figure 1.15 shows a diagram of the MALDI desorption ionization process.

MALDI is more sensitive than other laser ionization techniques. Indeed, the number of matrix molecules exceeds widely those of the analyte, thus separating the analyte molecules and thereby preventing the formation of sample clusters that inhibit the appearance of molecular ions. The matrix also minimizes sample damage from the laser pulse by absorbing most of the incident energy and increases the efficiency of energy transfer from the laser to the analyte. So the sensitivity is also highly increased. MALDI is also more universal than the other laser ionization techniques. Indeed, it is not necessary to adjust the wavelength to match the absorption frequency of each analyte because it is the matrix that absorbs the laser pulse. Furthermore, because the process is independent of the absorption properties and size of the compound to be analysed, MALDI allows the desorption and ionization of analytes with very high molecular mass in excess of 100 000 Da. For example, MALDI allows the detection of femtomoles of proteins with molecular mass up to 300 000 Da [29,30].

MALDI mass spectrometry has become a powerful analytical tool for both synthetic polymers and biopolymers [31]. Typical MALDI spectra include mainly the monocharged molecular species by protonation in positive ion mode. More easily deprotonated compounds are usually detected in negative ion mode. Some multiply charged ions, some
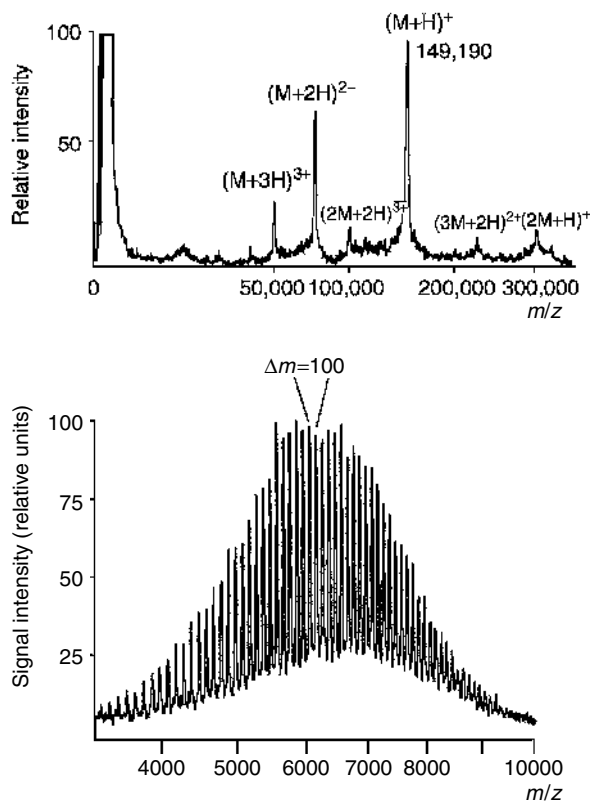
Figure 1.16
MALDI spectra of a monoclonal antibody (above) and of
a polymer PMMA 7100 (below). Reproduced (modified)
from Hillenkamp F.H. and Kras M., Meth. Enzymol.,
193, 280–295, 1990 and from Finnigan MAT documen-
tation, with permission.

multimers and very few fragments can also be observed. Compounds that are not easily
protonated can be cationized instead, often by adding a small quantity of alkali, copper or
silver cations to the sample. As MALDI spectra are simple, complex mixtures can be easily
analysed. Figure 1.16 shows the MALDI spectrum of a monoclonal antibody [32] of about
150 kDa. This figure also presents the MALDI spectrum of a synthetic polymer correspond-
ing to polymethyl methacrylate (PMMA 7100) with an average mass of about 7100 Da.

The use of MALDI to image biological materials is another interesting application
[33, 34]. Indeed, as with LD and SIMS, MALDI has been used to map the distribution of
targeted biomolecules in tissue. It allows for example the study of peptides, proteins and
other biomolecules directly on tissue sections.

Contrary to most other ionization sources that yield a continuous ion beam, MALDI is
a pulsed ionization technique that produces ions in bundles by an intermittent process. The
pulsed nature of the MALDI source is well suited for the time-of-flight (TOF) analyser. In
addition, the TOF analyser has the ability to analyse ions over a wide mass range and thus

Table 1.1 Some common lasers used for MALDI.

Laser	Wavelength	Energy (eV)	Pulse width
Nitrogen	337 nm	3.68	<1 ns to a few ns
Nd:YAG μ3	355 nm	3.49	5 ns
Nd:YAG μ4	266 nm	4.66	5 ns
Er:YAG	2.94 μm	0.42	85 ns
CO_2	10.6 μm	0.12	100 ns + 1 μs tail

can analyse the high-mass ions generated by MALDI. Altogether, this explains why most MALDI spectra have been obtained with MALDI-TOF spectrometers. However, there is no fundamental reason to limit the use of MALDI sources with TOF analysers. MALDI sources have also been coupled to other mass analysers, such as ion trap or Fourier transform mass spectrometers. These instruments allow MS/MS analysis to be performed much more powerfuly and easier realized than using TOF instruments. Furthermore, Fourier transform mass spectrometers reach high resolutions.

1.8.2 Practical Considerations

Among the different lasers used, UV lasers are the most common because of their ease of operation and their low price. N_2 lasers ($\lambda = 337$ nm) are considered as the standard, though Nd:YAG lasers ($\lambda = 266$ or 355 nm) are also used. MALDI can also use IR lasers like Er:YAG lasers ($\lambda = 2.94$ μm) or CO_2 lasers ($\lambda = 10.6$ μm). A summary of laser wavelengths and pulse widths usually used for MALDI is listed in Table 1.1. It is not the power density that is the most important parameter to produce significant ion current but the total energy in the laser pulse at a given wavelength [35]. Generally, the power density required corresponds to an energy flux of 20 mJ cm^{-2}. The pulse widths of lasers vary from a few tens of nanoseconds to a few hundred microseconds. The laser spot diameter at the surface of the sample varies from 5 to 200 μm. It is important to determine the threshold irradiance, the laser pulse power that results in the onset of desorption of the matrix. Molecular species of the analyte are generally observed at slightly higher irradiances but higher laser power leads to more extensive fragmentation and induces a loss of mass resolution.

MALDI spectra obtained with UV or IR lasers are essentially identical for most analysed samples. There are only very small differences. Indeed, when an IR laser is used, only less fragmentation is observed, indicating that the IR-MALDI is somewhat cooler. On the other hand, IR-MALDI induces a larger depth of vaporization per shot that leads to shorter lifetime of the sample. Compared with UV-MALDI, a somewhat lower sensitivity is observed.

Matrix selection and optimization of the sample preparation protocol are the most important steps in the analysis because the quality of the results depends on good sample preparation. However, the preparation procedures are still empirical. The MALDI matrix selection is based on the laser wavelength used. In addition, the most effective matrix is strongly related to the class of analyte and may differ for analytes that have apparently similar structures. The MALDI matrices must meet a number of requirements simultaneously. These are strong absorbance at the laser wavelength, low enough mass to be sublimable,

Table 1.2   Some common UV-MALDI matrices.

Analyte	Matrix	Abbreviation
Peptides/proteins	α-Cyano-4-hydroxycinnamic acid	CHCA
	2,5-Dihydroxybenzoic acid (gentisic)	DHB
	3,5-Dimethoxy-4-hydroxycinnamic acid (sinapic)	SA
Oligonucleotides	Trihydroxyacetophenone	THAP
	3-Hydroxypicolinic acid	HPA
Carbohydrates	2,5-Dihydroxybenzoic acid	DHB
	α-Cyano-4-hydroxycinnamic acid	CHCA
	Trihydroxyacetophenone	THAP
Synthetic polymers	Trans-3-indoleacrylic acid	IAA
	Dithranol	DIT
	2,5-Dihydroxybenzoic acid	DHB
Organic molecules	2,5-Dihydroxybenzoic acid	DHB
Inorganic molecules	Trans-2-(3-(4-tert-Butylphenyl)-2methyl-2-propenyliedene)malononitrile	DCTB
Lipids	Dithranol	DIT

vacuum stability, ability to promote analyte ionization, solubility in solvents compatible with analyte and lack of chemical reactivity. However, these general guidelines for matrix selection are not sufficient to predict a good matrix. Indeed, numerous matrix candidates have been inspected and their ability to function as a MALDI matrix has been exemplified, but only very few are good matrices.

Common UV-MALDI matrices are listed in Table 1.2 with the class of compounds with which they are used. The matrices used with IR lasers, such as urea, caboxylic acids, alcohols and even water, are often closer to the natural solutions than the highly aromatic UV-MALDI matrices. In addition, there are many more potential matrices for IR-MALDI owing to the strong absorption of molecular compounds at IR wavelengths, even if the correlation between ion formation and matrix absorption in IR-MALDI is not clear [36].

A number of different sample preparation methods have been described in the literature [37, 38]. A collection of these protocols is accessible on the Internet [39, 40]. The original method that is always the most widely used has been called dried-droplet. This method consists of mixing some saturated matrix solution (5–10 μl) with a smaller volume (1–2 μl) of an analyte solution. Then, a droplet (0.5–2 μl) of the resulting mixture is placed on the MALDI probe, which usually consists of a metal plate with a regular array of sites for sample application. The droplet is dried at room temperature and when the liquid has completely evaporated to form crystals, the sample may be loaded into the mass spectrometer.

MALDI suffers from some disadvantages such as low shot-to-shot reproducibility and strong dependence on the sample preparation method. Each laser shot ablates a few layers of the deposit at the spot where the laser irradiates. This can produce variation in the shot-by-shot spectrum. Also, the impact position on the surface of the deposit can lead to spectral variations. Improvement of the deposit homogeneity gives a better reproducibility of the signal. This is very important if precise quantitative results must be obtained. A given

position may become depleted after approximately 50 shots but a few laser shots are usually sufficient to acquire a reasonable spectrum. When a long and stable signal is needed, the target plate moves during spectra acquisition to expose fresh sample continuously to the laser irradiation spot.

MALDI is relatively less sensitive to contamination by salts, buffers, detergents, and so on in comparison with other ionization techniques [41]. The analyte must be incorporated into the matrix crystals. This process may generally serve to separate in solid phase the analyte from contaminants. However, high concentrations of buffers and other contaminants commonly found in analyte solutions can interfere with the desorption and ionization process of samples. Prior purification to remove the contaminants leads to improvements in the quality of mass spectra. For instance, the removal of alkali ions has proven to be very important for achieving high desorption efficiency and mass resolution.

On-probe purification using derivatized MALDI probe surfaces has been described to simplify the sample preparation process. Various developments in this field have allowed the introduction of new techniques such as the surface-enhanced laser desorption ionization (SELDI) [42]. The surface of the probe plays an active role in binding the analyte by hydrophobic or electrostatic interactions, while contaminants are rinsed away. In the same way, this technique uses targets with covalently coupled antibodies directed against a protein, allowing its purification from biological samples as urine or plasma. Subsequent addition of a droplet of matrix solution allows MALDI analysis.

In MALDI, the laser typically irradiates the analyte on the front side of an opaque surface (reflection geometry). Another configuration consisting of laser irradiation through the back of the sample (transmission geometry) has been used. However, the use of this configuration is limited. The sample consumption for MALDI is much lower than the amount required for analysis because only a small fraction of the surface of the sample on the MALDI probe is irradiated by the laser during the acquisition. After analysis, the remaining sample can be recovered for other experiments.

Matrix-free direct laser desorption ionization of analyte has been studied on different kinds of surfaces without real success because degradation of the sample is usually observed. However, good results were obtained with the method called surface-activated laser desorption ionization (SALDI) [43] which uses graphite as the surface. But the use of porous silicon as a new surface is more promising and has led to the development of a new method called desorption ionization on silicon (DIOS) [44]. Unlike the other matrix-free laser desorption ionization methods, DIOS allows ion formation from analyte with little or no degradation.

As already mentioned, DIOS is a matrix-free method that uses pulsed laser desorption ionization on porous silicon. Indeed, this method simply consists of depositing the sample in solution on porous silicon, without any added organic matrix. The structure of porous silicon allows the analyte molecules to be retained while its strong UV absorption allows the desorption ionization of the sample under UV laser irradiation. DIOS has most of its characteristics in common with MALDI but has several advantages to MALDI because it does not use a matrix. DIOS mass spectra do not present interference in the low-mass range, while signals due to the matrix are observed in MALDI. It allows small molecules to be easily analysed. For the same reason, the deposition of the sample in aqueous solution is uniform and the preparation of the sample is simplified. Furthermore, DIOS is equivalent to MALDI in sensitivity, but is more tolerant of the presence of salts or buffers. This method is useful for a large range of small-size compounds (100–3000 Da) such as organic

compounds or biomolecules including peptides and oligosaccharides. With all of these characteristics, DIOS is a complementary ionization method to MALDI.

1.8.3 Fragmentations

The MALDI process can lead to fragmentations that occur as a result of the excess energy that is imparted to the analyte during the desorption ionization process. There are essentially three different types of fragmentations that generate fragment ions in MALDI spectra. These fragmentations are discriminated according to the place where they occur.

Fragmentations taking place in the source are called in-source decay (ISD) fragmentations. To be precise, fragmentation at the sample surface that occurs before or during the desorption event (on a time scale of a few picoseconds to nanoseconds) is called prompt fragmentation. Fragmentation occurring in the source after the desorption event but before the acceleration event (on a time scale of a few nanoseconds to microseconds) is called fast fragmentation. Fragmentation that occurs after the acceleration region of the mass spectrometer is called post-source decay (PSD) fragmentation. It corresponds to the fragmentation of metastable ions, which are stable enough to leave the source but contain enough excess energy to allow their fragmentation before they reach the detector.

There are many mechanisms involved in the activation of ions produced in MALDI. Acquisition of an excess of internal energy can be due to the direct interaction photon/molecule, to ionization energy and to activation of molecules in solid state. Another important mechanism consists of the multiple collisions that ions undergo in the source. Indeed, the laser pulse provokes expansion of the matrix into the gas phase, carrying intact analyte in the expanding matrix plume. Desorption of these small molecules induces the formation of a very dense cloud of neutral molecules located just over the surface. The acceleration of the ions through this cloud during their extraction from the source causes many collisions that increase their internal energy. These collisions can be controlled by the strength of the electric field used to extract the ions from the source. By increasing the electric field, the ion-neutral collision energy is increased and thus the internal energy of the ions increases too. On the other hand, the internal energy of the ions increases less in a weaker electric field because the collision energy decreases in the expanding cloud.

ISD fragmentations lead to product ions that are always apparent in the MALDI spectra, whereas the observation of product ions from PSD fragmentation needs certain instrumental conditions. For example, a MALDI source coupled to a linear TOF analyser allows detection of fragment ions produced in the source at their appropriate m/z ratio. On the contrary, fragment ions produced after the source cannot be resolved from their precursor ions and are detected at the same apparent m/z ratio. This induces a broadening of the peaks with a concomitant loss of mass resolution and sensitivity.

1.8.4 Atmospheric Pressure MALDI

In 2000, various developments in the field of MALDI led to the advent of new methods such as the atmospheric pressure MALDI (AP-MALDI) source. This method combines the atmospheric pressure (AP) source and MALDI [45–47]. Indeed, this source produces ions of analytes under normal atmospheric pressure conditions from analyte-doped matrix microcrystals by irradiating these crystals with laser pulses.
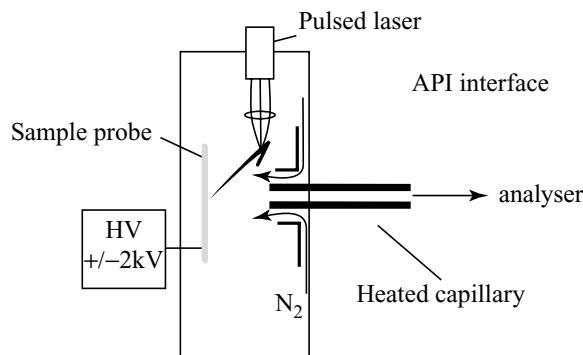
Figure 1.17
Diagram of an AP-MALDI source. Ions are transferred
into the mass analyser using the atmospheric pressure
interface.

The AP-MALDI source is illustrated in Figure 1.17. It works in a similar manner to
the conventional MALDI source. The same sample preparation techniques and the same
matrices used for conventional vacuum MALDI can be used successfully for AP-MALDI.
The main difference is the pressure conditions where ions are produced. Conventional
MALDI is a vacuum ionization source where analyte ionization takes place inside the
vacuum of the mass spectrometer whereas AP-MALDI is an atmospheric ionization source
where ionization occurs under atmospheric pressure conditions outside of the instrument
vacuum.

The ions are transferred into the vacuum of the mass analyser using an atmospheric
pressure interface (API). To assist the transport of ions produced from the atmospheric
pressure ionization region towards the high vacuum, a high voltage (typically, 2–3 kV) is
applied on the surface of the target plate (MALDI probe) and a stream of dry nitrogen
is applied to the area surrounding the target plate. As the transfer of ions into the mass
spectrometer is relatively inefficient, the total sample consumption is higher for AP-MALDI
than for vacuum MALDI. However, sensitivity of this ion source is not decreased because
the sample consumption for MALDI is much lower than the amount required for analysis.
Indeed, a large fraction of the sample is not used during data acquisition.

The mechanism of AP-MALDI ion production is similar to that of conventional MALDI.
Thus, the AP-MALDI source, like the conventional MALDI source, produces mainly
monocharged molecular species but with a narrower mass range. But, because of the
fast and efficient thermalization of the ion internal energy at atmospheric conditions, AP-
MALDI is a softer ionization technique compared with conventional vacuum MALDI and
even softer than vacuum IR-MALDI. Ions produced by this method generally exhibit no
fragmentation but tend to form clusters with the matrix. These unwanted adducts between
matrix and analyte can be eliminated by increasing the energy transferred to the ions in the
source. For instance, increasing the laser energy or some API parameters, such as capillary
temperature, increases the analyte-matrix dissociation process.

The advantages of AP-MALDI include those advantages typically associated with a
MALDI source but without some of the drawbacks. Indeed, AP-MALDI does not require
a vacuum region and is decoupled from the mass analyser, allowing it to be coupled with
any mass spectrometer equipped with API. It is also easily interchangeable with other

atmospheric pressure sources, such as electrospray ionization (see later). As a result of the almost complete decoupling of the ion desorption from the mass analyser, the performance of the instrument (calibration, resolution and mass accuracy) is not affected by source conditions (type of sample matrix, sample preparation method and location of the laser spot on the sample). This allows much greater experimental flexibility. It is possible, for instance, to use long-pulse lasers to increase the overall sensitivity without observing deterioration in resolution. AP-MALDI sources, like the conventional MALDI source, can be used to image biological materials. But sampling at atmospheric pressure allows the examination of samples that are vacuum sensitive, such as samples containing volatile solvents. This method can be easily applied to spatial analysis of native surfaces of biological tissues.

1.9 Thermospray

The principle of the thermospray (TSP), proposed by Blakney and Vestal [48, 49] in 1983, is shown in Figure 1.18.

A solution containing a salt and the sample to be analysed is pumped into a steel capillary, which is heated to high temperature allowing the liquid to heat quickly. The solution passes through a vacuum chamber as a supersonic beam. A fine-droplet spray occurs, containing ions and solvent and sample molecules. The ions in the solution are extracted and accelerated towards the analyser by a repeller and by a lens focusing system. They are desorbed from the droplets carrying one or several solvent molecules or dissolved compounds. It is thus not necessary to vaporize before ionization: ions go directly from the liquid phase to the vapour phase. To improve the ion extraction, the droplets at the outlet of the capillary may be charged by a corona discharge. The droplets remain on their supersonic trip to the outlet where they are pumped out continuously through an opening located in front of the supersonic beam. Large vapour volumes from the solvent are thus avoided.
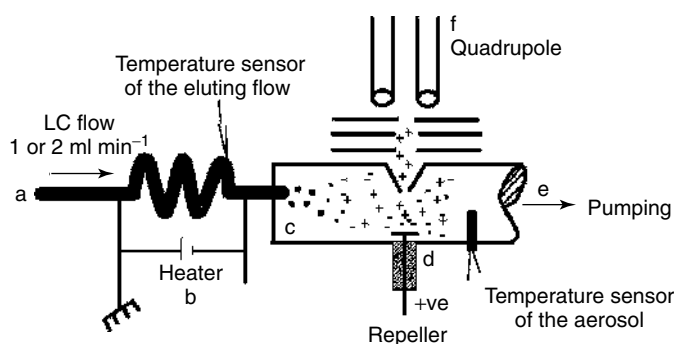
Figure 1.18
Diagram of a thermospray source. The chromatographic effluent comes in at (a) the transfer line is suddenly heated at (b) and the spray is formed under vacuum at (c). At (d) the spray goes between a pusher with a positive potential and a negative cone for positive ions. The ions are thus extracted from the spray droplets and accelerated towards the spectrometer (f). At (e), a high-capacity pump maintains the vacuum.

In order to avoid the freezing of the droplets under vacuum, the liquid must be heated during the injection. This heating is programmed by feedback from a thermocouple which measures the beam temperature under vacuum. The heating is achieved by having a current pass through the capillary that carries the liquid and thus also acts as a heating resistance.

1.10 Atmospheric Pressure Ionization

Besides AP-MALDI, already described earlier, electrospray (ESI), atmospheric pressure chemical ionization (APCI), atmospheric pressure photoionization ionization (APPI), DESI and DART are other examples of atmospheric pressure ionization (API) sources.

Such sources ionize the sample at atmospheric pressure and then transfer the ions into the mass spectrometer. An atmospheric pressure interface is then used to transfer ions into the high vacuum of the mass analyser. The problem lies in coupling an atmospheric pressure source compartment with an analyser compartment that must be kept at a very low pressure or at a very high vacuum (10^{-5} Torr).

This problem is solved by adopting a differential pumping system. Usually two intermediate vacuum compartments are used between the source compartment and the analyser compartment because the pressure difference is quite large. The compartments are connected between them by lenses with very small orifices (called skimmers or cones). The pressures of the intermediate vacuum compartments are gradually reduced by using several differential stages of high-capacity pumps. Ions go across the compartments in the order of higher to lower pressure through these small orifices to reach the analyser compartment. This orifice must be wide enough to allow the introduction of as many ions as possible in order to enhance the sensitivity. But, on the other hand, the orifice must not be too wide to maintain a correct vacuum in the analyser compartment. A transfer optics system including focusing lenses or focusing multipole lenses is provided in the intermediate-vacuum compartments to inject ions effectively into the orifices. The scheme of an atmospheric pressure interface is illustrated in Figure 1.19.

Another problem lies in the cooling caused by the sample and the solvent adiabatic expansion that favours the appearance of ion clusters. Consequently, ion desolvation is also an important aspect of atmospheric pressure interface design. Efficient desolvation is provided by the introduction of a heated metallized transfer tube (about $200°C$) or by applying a counter-current flow of heated dry gas also called curtain gas. The desolvation is also improved by accelerating the ions in a region of the interface where the pressure is in the millibar range. The acceleration is obtained by applying a voltage between the different
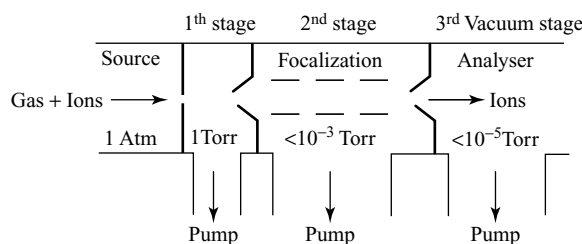
Figure 1.19
Scheme of an atmospheric interface with differential pumping system using three stages.

extraction lenses. The ions collide with residual gas molecules, increase their internal energy, which induces their final desolvation, and the ion clusters disappear. However, these collisions can also give enough energy to induce ion fragmentation. This kind of fragmentation is called in-source fragmentation. The desolvation should be maximized to get a gain in sensitivity because the distribution of an analyte in different species, which are clusters, leads to a decrease in detection sensitivity. Furthermore, the formation of clusters should be controlled when doing quantitative analysis because the analyte of interest should be in a well-defined and stable form.

The transfer of ions from atmospheric pressure to the vacuum of a spectrometer necessarily induces ion losses. But these losses are compensated by the higher total ion yield in the API source due to fast thermal stabilization at atmospheric conditions. Indeed, when the sample ionization is performed under atmospheric pressure [50,51], an ionization efficiency 10^3 to 10^4 times as great as in a reduced-pressure CI source is obtained.

The early API source designs used an axial configuration. The ions were produced in the axis of the orifice. Designs have changed, however. Now the orthogonal configuration to introduce the ions into the interface is used in many API sources. The main advantage is that the orifice is no longer saturated by solvent. Instead, only ions are directed towards the inlet. Consequently, orifices can be larger than in the axial configuration. The combination of larger orifices and noise reduction largely compensates for transmission losses due to the orthogonal geometry, giving a large gain in sensitivity. Another advantage of this configuration is that the flow rates can be increased. Furthermore, this configuration gives better protection of the orifice against contamination or clogging, giving a gain in robustness. However, the orthogonal configuration with indirect trajectory of analyte ions also introduces unwanted discrimination based on mass or charge.

The most important advantage of API sources is the simplicity for the direct on-line coupling of separation techniques (HPLC, CE, etc.) to the mass spectrometer. Another attractive aspect of these sources is the easy introduction of the sample into a mass spectrometer because the operation at atmospheric pressure outside of the mass spectrometer eliminates the complicated procedure of introducing the sample into its high vacuum.

1.11 Electrospray

In the literature, electrospray is abbreviated to either ESI or ES. Because ES is ambiguous, we prefer to use ESI. The success of ESI started when Fenn *et al.* [52, 53] showed that multiply charged ions were obtained from proteins, allowing their molecular weight to be determined with instruments whose mass range is limited to as low as 2000 Th. At the beginning, ESI was considered as an ionization source dedicated to protein analysis. Later on, its use was extended not only to other polymers and biopolymers, but also to the analysis of small polar molecules. It appeared, indeed, that ESI allows very high sensitivity to be reached and is easy to couple to high-performance liquid chromatography HPLC, μHPLC or capillary electrophoresis. ESI principles and biological applications have been extensively reviewed [54–56]. Several edited books on this subject also appeared in 1996 and 1997 [57, 58].

ESI [59–64] is produced by applying a strong electric field, under atmospheric pressure, to a liquid passing through a capillary tube with a weak flux (normally 1–10 μl min^{-1}). The electric field is obtained by applying a potential difference of 3–6 kV between this capillary and the counter-electrode, separated by 0.3–2 cm, producing electric fields of the
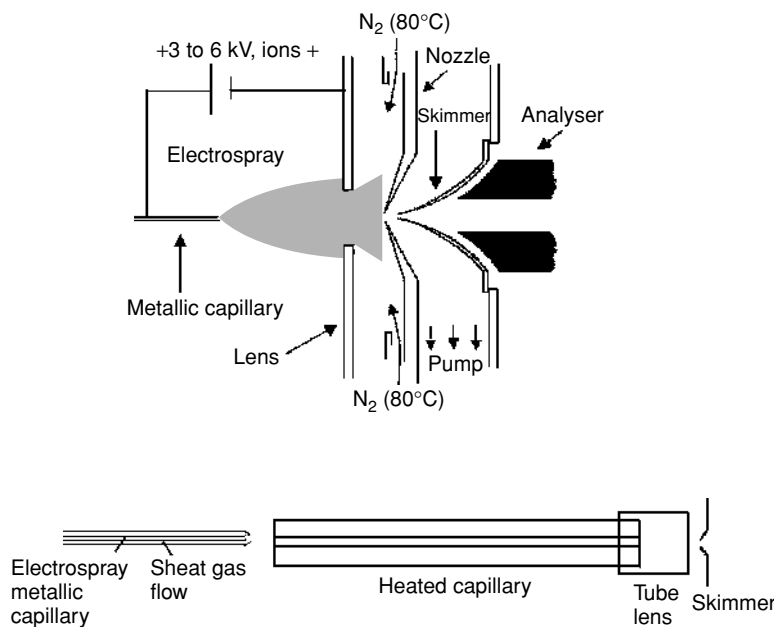
Figure 1.20
Diagram of electrospray sources, using skimmers for ion focalization and
a curtain of heated nitrogen gas for desolvation (top), or with a heated
capillary for desolvation (bottom).

order of 10^6 V m^{-1} (Figure 1.20). This field induces a charge accumulation at the liquid
surface located at the end of the capillary, which will break to form highly charged droplets.
A gas injected coaxially at a low flow rate allows the dispersion of the spray to be limited
in space. These droplets then pass either through a curtain of heated inert gas, most often
nitrogen, or through a heated capillary to remove the last solvent molecules.

The spray starts at an 'onset voltage' that, for a given source, depends on the surface
tension of the solvent. In a source which has an onset voltage of 4 kV for water (surface ten-
sion 0.073 N m^{-2}), 2.2 kV is estimated for methanol (0.023 N m^{-2}), 2.5 kV for acetonitrile
(0.030 N m^{-2}) and 3 kV for dimethylsulfoxide (0.043 N m^{-2}) [65]. If one examines with a
microscope the nascent drop forming at the tip of the capillary while increasing the voltage,
as schematically displayed in Figure 1.21, at low voltages the drop appears spherical, then
elongates under the pressure of the accumulated charges at the tip in the stronger electric
field; when the surface tension is broken, the shape of the drop changes to a 'Taylor cone'
and the spray appears.

Gomez and Tang [66] were able to obtain photographs of droplets formed and dividing
in an ESI source. A drawing of a decomposing droplet is displayed in Figure 1.22. From
their observations, they concluded that breakdown of the droplets can occur before the limit
given by the Rayleigh equation is reached because the droplets are mechanically deformed,
thus reducing the repulsion necessary to break down the droplets.

The solvent contained in the droplets evaporates, which causes them to shrink and
their charge per unit volume to increase. Under the influence of the strong electric field,

Figure 1.21
Effect of electrospray potential on the drop at the tip of the capillary, as observed with binoculars while increasing the voltage. Left: at low voltage, the drop is almost spherical. Centre: at about 1 or 2 kilovolts, but below the onset potential, the drop elongates under the pressure of the charges accumulating at the tip. Right: at onset voltage, the pressure is higher than the surface tension, the shape of the drop changes at once to a Taylor cone and small droplets are released. The droplets divide and explode, producing the spray.
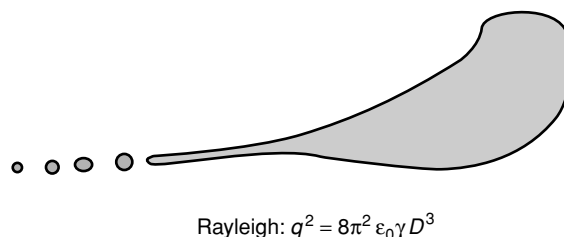
Rayleigh: $q^2 = 8\pi^2 \varepsilon_0 \gamma D^3$

Figure 1.22
A decomposing droplet in an electrospray source, according to [66]; q, charge; ε_0, permittivity of the environment; γ, surface tension and D, diameter of a supposed spherical droplet.

deformation of the droplet occurs. The droplet elongates under the force resulting from the accumulation of charge, similarly to what occurred at the probe tip, and finally produces a new Taylor cone. From this Taylor cone, about 20 smaller droplets are released. Typically a first-generation droplet from the capillary will have a diameter of about 1.5 μm and will carry around 50 000 elementary charges, or about 10^{-14} C. The offspring droplets will have a diameter of 0.1 μm and will carry 300 to 400 elementary charges. The total volume of the offspring droplets is about 2 % of the precursor droplet but contain 15 % of the charge. The charge per unit volume is thus multiplied by a factor of seven. The precursor droplet will shrink further by solvent evaporation and will produce other generations of offspring.

These small, highly charged droplets will continue to lose solvent, and when the electric field on their surface becomes large enough, desorption of ions from the surface occurs [65]. Charges in excess accumulate at the surface of the droplet. In the bulk, analytes as well as electrolytes whose positive and negative charges are equal in number are present at a somewhat higher concentration than in the precursor droplet. The desorption of charged molecules occurs from the surface. This means that sensitivity is higher for compounds whose concentration at the surface is higher, thus more lipophilic ones. When mixtures of compounds are analysed, those present at the surface of droplets can mask, even completely, the presence of compounds which are more soluble in the bulk. When the droplet contains very large molecules, like proteins for example, the molecules will not desorb, but are freed by evaporation of the solvent. This seems to occur when the molecular weight of the compounds exceeds 5000 to 10 000 Da.

The ions obtained from large molecules carry a greater number of charges if several ionizable sites are present. Typically, a protein will carry one charge per thousand daltons
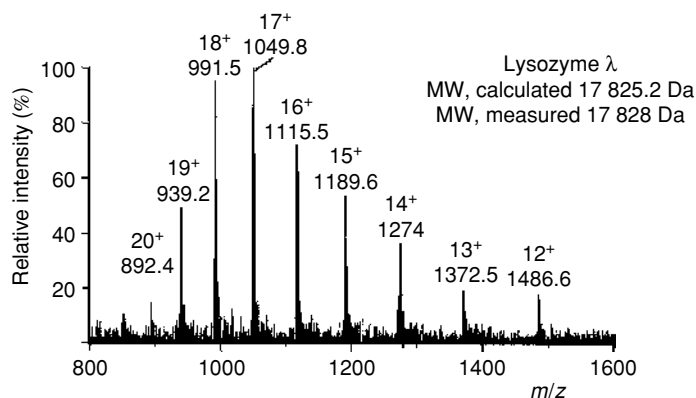
Figure 1.23
ESI spectrum of phage λ lysozyme; m/z in Th and the number of
charges are indicated on each peak. The molecular mass is measured
as being $17\,828 \pm 2.0$ Da.

approximately, less if there are very few basic amino acids. As an example, the ESI
spectrum of phage lambda lysozyme is shown in Figure 1.23. Small molecules, say less
than a thousand daltons, will produce mainly monocharged ions. ESI can also be used in the
case of molecules without any ionizable site through the formation of sodium, potassium,
ammonium, chloride, acetate or other adducts.

ESI has important characteristics: for instance, it is able to produce multiply charged ions
from large molecules. The formation of ions is a result of the electrochemical process and of
the accumulation of charge in the droplets. The ESI current is limited by the electrochemical
process that occurs at the probe tip and is sensitive to concentration rather than to total
amount of sample.

1.11.1 Multiply Charged Ions

Large molecules with several ionizable sites produce by ESI multiply charged ions, as
shown for lysozyme positive ions in Figure 1.23.

Obtaining multiply charged ions is advantageous as it improves the sensitivity at the
detector and it allows the analysis of high-molecular-weight molecules using analysers with
a weak nominal mass limit. Indeed, the technical characteristics of mass spectrometers are
such that the value being measured is not the mass, but the mass-to-charge ratio m/z.

The ESI mass spectra of biological macromolecules normally correspond to a statistical
distribution of consecutive peaks characteristic of multiply charged molecular ions obtained
through protonation $(M + zH)^{z+}$, or deprotonation $(M - zH)^{z-}$, with minor if any contri-
butions of ions produced by dissociations or fragmentations. However, as the measured
apparent mass is actually m/z, to know m one needs to determine the number of charges z.

Consider a positive ion with charge z_1 whose mass-to-charge ratio is measured as being
m_1 Th, issued from a molecular ion with mass M Da to which z_1 protons have been added.
We then have

$$z_1 m_1 = M + z_1 m_p$$

where m_p is the mass of the proton.
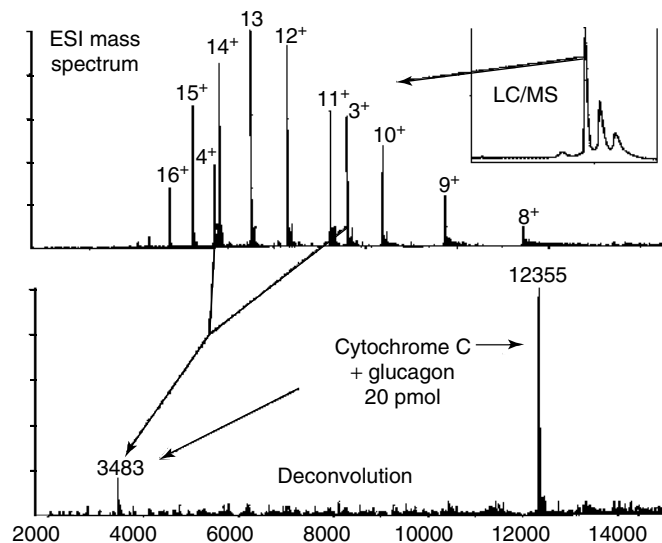
Figure 1.24
Deconvolution of an ESI spectrum of a protein mixture. From
Finnigan documentation. Reprinted, with permission.

An ion separated from the first one by $(j-1)$ peaks, in increasing order of mass-to-charge
ratio, has a measured ratio of m_2 Th and a number of charges $z_1 - j$, so that

$$m_2(z_1 - j) = M + (z_1 - j)m_p$$

These two equations lead to

$$z_1 = \frac{j(m_2 - m_p)}{(m_2 - m_1)} \quad \text{and} \quad M = z_1(m_1 - m_p)$$

In the case of negative multiply charged ions, analogous equations lead to

$$z_1 = \frac{j(m_2 + m_p)}{(m_2 - m_1)} \quad \text{and} \quad M = z_1(m_1 + m_p)$$

In the example shown in Figure 1.23 using the peaks at m/z 939.2 and 1372.5 ($j = 6$),
we obtain $z_1 = 6(1372.5 - 1.0073)/(1372.5 - 939.2) = 19$ and we can number all the peaks
measured according to the number of charges. M can be calculated from their mass. The
average value obtained from all of the measured peaks is 17 827.9 Da with a mean error
of 2.0 Da. This technique allowed the determination of the molecular masses of proteins
above 130 kDa with a detection limit of about 1 pmol using a quadrupole analyser.

A variety of algorithms have been developed to allow the determination of the molecular
mass through the transformation of the multiply charged peaks present in the ESI spectrum
into singly charged peaks. Some of them also allow the deconvolution ESI spectra of
mixtures, as is shown in Figure 1.24. However, the complexity of the spectra obtained for
a single compound is such that only simple mixtures can be analysed.
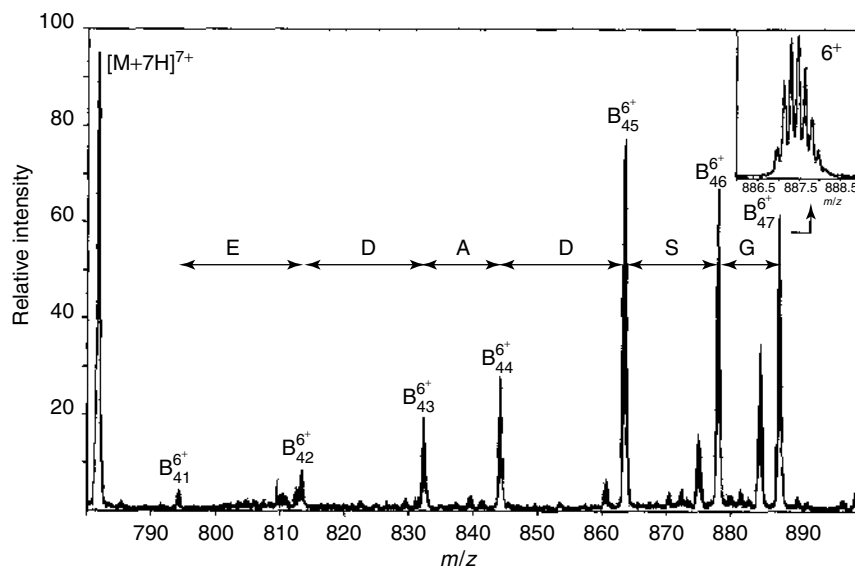
Figure 1.25
Product ion spectrum of the $[M + 7H]^{7+}$ ion from the following peptide: ALVRQG-LAKVAYVYKPNNTHEQHLRKSEAQAKKEKLLNIWSEDNADSGQ. Notice that fragment ions having lower charge number z may appear at higher m/z values than the precursor, which indeed occurs in the spectrum shown. The inset shows that, owing to the high resolution, the isotopic peaks are observed separated by 1/6 Th, and thus $1/z = 1/6$ or $z = 6$. From Andersen J., Molina H., Moertz E., Krogh T.N., Chernuchevich I., Taylor L., Vorm O. and Mann M., 'Quadrupole-TOF Hybrid Mass Spectrometers Bring Improvements to Protein Indentification and MS/MS Analysis of Intact Proteins' The 46th Conference on Mass Spectrometry and Allied Topics, Orlando, Florida, 1998, p. 978. Reprinted, with permission.

At high resolution, the individual peaks with different charge states observed at low resolution are each split into several peaks corresponding to the isotope distribution. As neighbour peaks differ by 1 Da, the observed distance between them will be $1/z$, allowing the direct determination of the charge state of the corresponding ion. This is important for MS/MS spectra of multiply charged ions, as the preceding rules to assign the z value can no longer be applied. An example is displayed in Figure 1.25 [67].

The ability of this ionization method for the determination of very high molecular weights is illustrated in Figure 1.26 [68]. The spectrum displayed is obtained from assemblies of vanillyl alcohol oxidase containing respectively 16 and 24 proteins. The spectrum was obtained with a hybrid quadrupole TOF instrument, Q-TOF Micromass, equiped with a micro-ESI source. To obtain such a spectrum one needs not only a mass spectrometer with sufficient mass range and resolution, but also high skill in protein purification.

1.11.2 Electrochemistry and Electric Field as Origins of Multiply Charged Ions

Charges of ions generated by ESI do not reflect the charge state of compounds in the analysed solution, but are the result of both charge accumulation in the droplets and charge
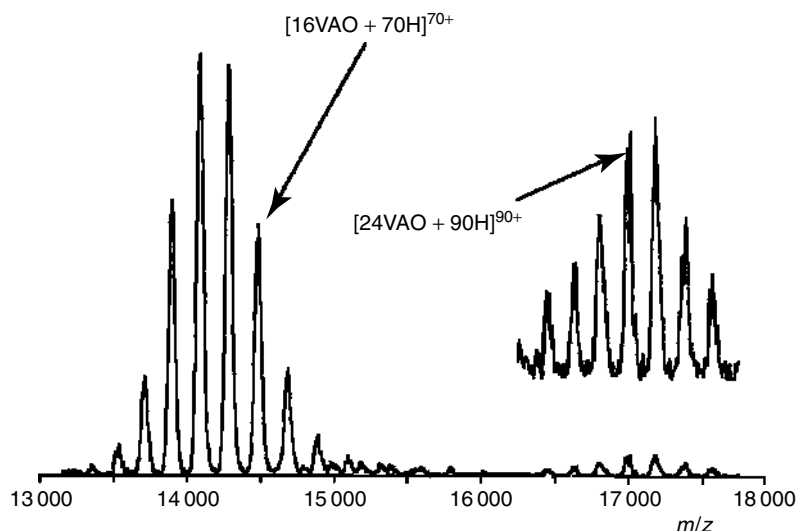
Figure 1.26
MicroESI Q-TOF spectrum of assemblies of vanillyl alcohol oxidase obtained by W.J.H. van Berkel and co-workers [68]. At the left, an octamer–dimer of 1.02 MDa molecular weight, and at the right, the octamer–trimer of 1.53 MDa. Reproduced courtesy of Dr. A.J.R. Heck.

modification by electrochemical process at the probe tip. This is clearly demonstrated by a convincing experiment reported by Fenselau and co-workers, and illustrated in Figure 1.27 [69]. They showed that negative ions of myoglobin can be observed at pH 3, while a calculation based on known pK values predicts that only 1 molecule per 3500 approximately would have one negative charge in the original solution. The results point out the role of the charge accumulation in droplets under the influence of the electric field on the formation of multiply charged ions. Furthermore, the 'pumping out' of the negative charges can only be performed if, at the same time, the same number of positive charges is electrochemically neutralized at the probe tip.

Moreover, it is worth noting that the negative ion spectrum of myoglobin at pH 3 shows a better signal-to-noise ratio than the same spectrum at pH 10 (Figure 1.27). This results from the fact that protons have a high electrochemical mobility, and is the first indication of the importance of the reduction process, when negative ions are analysed, that occurs at the probe tip.

At pH 10, positive ions can be observed too. Additional peaks in the spectra result from a modification of the protein at basic pH (loss of heme group).

Thus, it is worthy of consideration to try to acidify a solution with a view to a better detection of negative ions, and vice versa. Indeed, both H_3O^+ and OH^- have high limit equivalent conductivities, as shown in Table 1.3.

1.11.3 Sensitivity to Concentration

Another feature of ESI is its sensitivity to concentration, and not to the total quantity of sample injected in the source, as is the case for most other sources. This is shown in
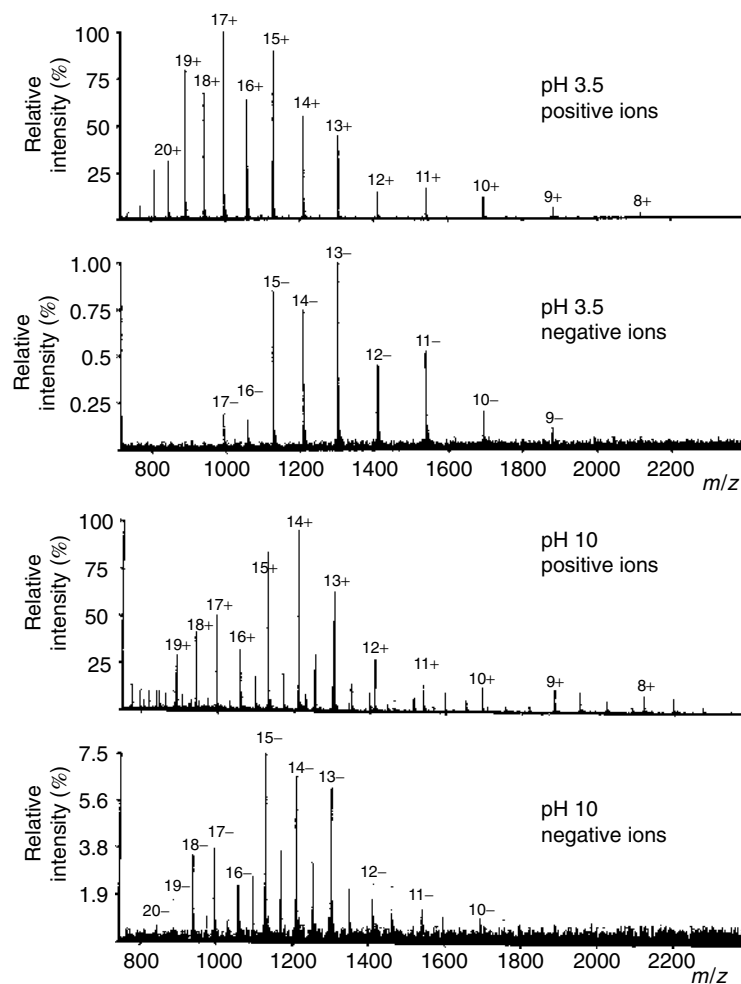
Figure 1.27
ESI spectra of myoglobin have been acquired in the positive and negative
ion mode, at pH 3 and at pH 10. At pH 3, negative ions are observed,
the most intense ions bearing from 13 to 15 charges. A calculation based
on known pK values shows that in the original solution, only 1 molecule
in approximately 3500 bears one negative charge. From Kelly M.A.,
Vestling M.M., Fenselau C. and Smith P.B., Org. Mass Spectrom., 27,
1143, 1992. Reproduced, with permission.

Figure 1.28 [70]. The intensity of the signals from the two monitored compounds is
measured while injecting the total flow from an HPLC column, $400\ \mu l\ min^{-1}$, or a part
of this flow, after splitting. As can be seen, the sensitivity increases somewhat when the
flow entering the source is reduced. This remains true up to flows as low as some tens
of nanolitres per minute. When flow rates higher than about $500\ \mu l\ min^{-1}$ are used, the
sensitivity is reduced. Lower flow rates also allow less analyte and buffer to be injected
in the source, reducing contamination. Furthermore, for the same amount of sample, an

Table 1.3 Some values of equivalent conductivity.

Cation	$\lambda_0{}^+$	Anion	$\lambda_0{}^-$
H_3O^+	350	OH^-	200
$NH_4{}^+$	74	Br^-	78
K^+	74	I^-	77
Na^+	50	Cl^-	76
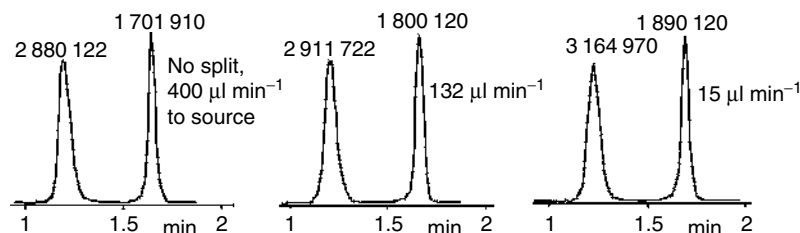
Figure 1.28
HPLC on a 2.1 mm column at 400 μl min^{-1} flow. Two drugs are monitored by selected ion monitoring. Left: 400 μl min^{-1} is injected in the source. Centre: 132 μl min^{-1} is split to the source. Right: 15 μl min^{-1} is split to the source. The integration values are displayed on top of the peaks and show that at reduced flow rates the sensitivity is slightly increased. Reproduced with data from Covey T., 'Analytical Characteristics of the Electrspray Ionization Process' pp. 21–59 in 'Biochemical and Biotechnological Applications of Eletrospray Ionization Mass Spectrometry' Snyder A.P., ed., ACS Symposium Series 619, American Chemical Society, 1996.

HPLC column with a lower diameter, and using smaller flow rates, will give an increased sensitivity because the concentration of the sample in the elution solvent is increased.

Based on this concentration dependence, modifications of the technique, called microelectrospray (μESI), or nanospray (nESI), which use much lower flow rates down to some tens of nanolitres per minute, have been developed using adapted probe tips [71–73]. Detection limits in the range of attomoles (10^{-15} moles) injected have been demonstrated.

1.11.4 Limitation of Ion Current from the Source by the Electrochemical Process

As may be seen from the electric circuit in Figure 1.29, when positive ions are extracted for analysis, electrons have to be provided in the circuit from the capillary. This will occur through oxidation of species in the solution at the capillary tip, mainly ions having a sufficient mobility. In other words, the same number of negative charges must be 'pumped' out of the solution as positive charges are extracted to the analyser. Thus, ESI is truly an electrochemical process, with its dependence on ion concentration and mobility as well as on polarization effects at the probe tip. For the detection of positive ions, electrons have to be provided by the solution, and thus an oxidation occurs. For negative ions, electrons
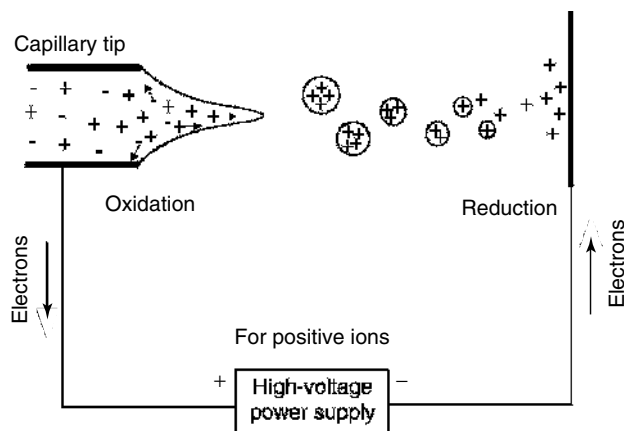
Figure 1.29
Schematic representation of electrochemical process in ESI.

have to be consumed, and thus a reduction occurs. These electrochemical reactions occur in the last micrometres of the metallic capillary. A major consequence is that the total number of ions per unit time that can be extracted to the spectrometer is actually limited by the electric current produced by the oxidation or reduction process at the probe tip. This limiting current is not dependent on the flow rate, up to very low flow, and this explains why ESI is only concentration dependent. In practice, the total ion current is limited to a maximum of about 1 μA.

In ESI, the number of variables is large, including nature of the solvent, flow, nature and size of the capillary, distance to the counter-electrode, applied potentiel, and so on. Furthermore, the ionization process includes many parameters, such as surface tension, nature of analyte and electrolytes, presence or not of other analytes, electrochemical processes at the probe tip, and so on.

Furthermore, the ESI source is a constant-current electrochemical cell [74]. Figure 1.30 shows the analogy between a classical constant-current electrochemical cell and an ESI source. The important consequence is that there will be a constant current I_M carried by the ions. If there are too many ions from salts in the flow, they will suffice to produce I_M and the ions of the sample will be either at low abundances or not observed. On the other hand, if the solution is very dilute and at very low flow (below 1 μl), the ion flow from the capillary can be insufficient to provide I_M. The electrochemical process at the probe tip will then produce additional ions by oxidation (or reduction in negative ion mode) of either the solvent or the sample depending on their respective oxidation (reduction) potentials. This will lead to the observation of radical cations or radical anions in the spectrum.

A paper by Fenn *et al*. [75] makes a critical comparison of the various theories about ESI. A simplified theory will be presented here for the relation between analyte concentration and abundances of the ions.

Ions, either positive or negative, of an analyte *A* will be desorbed from the droplets, producing a theoretical ion current $I_A = k_A[A]$, where k_A is a rate constant depending on the nature of *A*. Let us suppose that another ion *B* is produced from the buffer, at a rate $I_B = k_B[B]$, and that no other ions are sprayed. The total ion current for these two ions
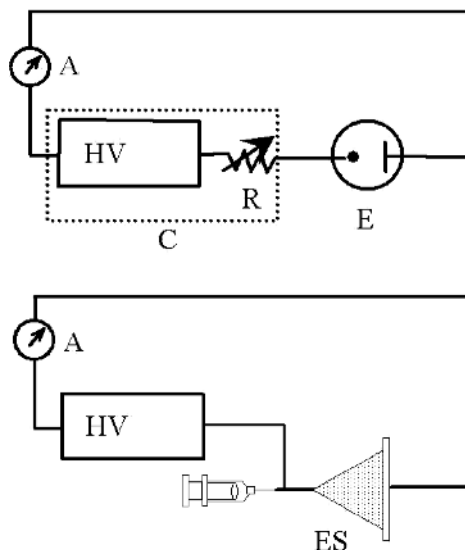
Figure 1.30
Top: scheme of a classical constant-current
electrochemical cell, combining a high-voltage
power supply with a large resistance. Bottom,
an ESI source. The large resistance results here
from the ion flow in the air. Reproduced with
data from Van Berkel G.J. and Zhou F., Anal.
Chem., 67, 2916, 1995.

is $I_T = (I_A + I_B)$, but this total ion current is limited by the oxidation, if positive ions
are desorbed, or reduction process that occurs at the probe tip. This limiting current is
symbolized I_M, and $I_T = I_M$ if no other ionic species are present.

The current for each ion will be proportional to its relative desorption rate, and the
pertinent equations are

$$I_A = I_M \frac{k_A [A]}{k_A [A] + k_B [B]} \qquad I_B = I_M \frac{k_B [B]}{k_A [A] + k_B [B]} \tag{1.1}$$

Let us consider that $[B]$ remains constant, but the analyte concentration $[A]$ varies; then
two limiting cases are to be considered. First, for $k_A[A] \gg k_B[B]$,

$$I_A \approx I_M \frac{k_A [A]}{k_B [B]} \qquad I_B \approx I_M \frac{k_B [B]}{k_B [B]} \approx I_M \tag{1.2}$$

This means that the intensity detected for A will be proportional to its concentration, but
the sensitivity will be inversely proportional to $[B]$.

The other extreme case leads to

$$I_A \approx I_M \frac{k_A [A]}{k_A [A]} \approx I_M \qquad I_B \approx I_M \frac{k_B [B]}{k_A [A]} \tag{1.3}$$

I_A remains constant, and quantitation of $[A]$ is no longer possible. The intensity of the signal
for B will become weaker as $[A]$ increases.
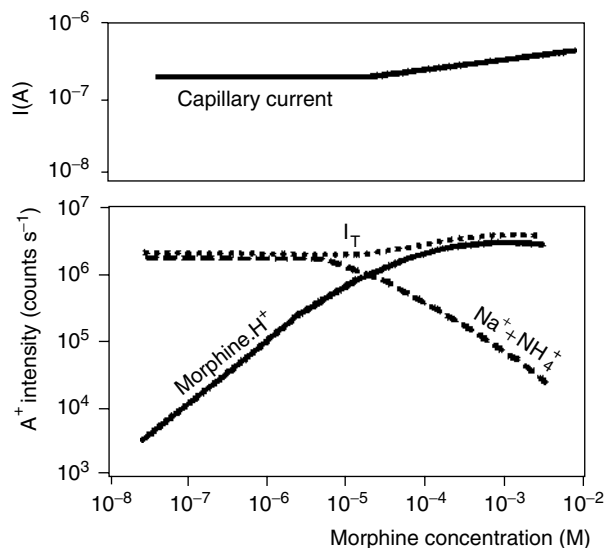
Figure 1.31
Influence of concentration on observed ion abundances, when increasing concentrations of morphine.HCl is injected in a solvent containing a constant concentration of sodium and ammonium salts. Linearity is observed at low concentrations, but from about 5×10^{-6} significant curvature is observed (note that the scales are logarithmic). At still higher concentrations, the intensity levels out. Reproduced (modified) from Kebarle P. and Tang L., Anal. Chem., 65, 972A, 1993.

This is shown by an experimental example from [65] in Figure 1.31. In a solvent containing NH_4^+ and Na^+ ions at constant concentrations, an increasing amount of morphine chlorhydrate is added. The graph shows on top the number of amperes at the capillary tip, and below the intensity monitored at the mass of protonated morphine and the sum of the intensities for the NH_4^+ and Na^+ ions. At low concentrations of morphine chlorhydrate, Equation (1.2) pertains, and linearity towards morphine concentration is observed. At high concentrations, the intensity for morphine is constant, and the signal for the other ions diminishes, in agreement with Equation (1.3). At intermediate values, the general Equation (1.1) applies.

1.11.5 Practical Considerations

To observe a stable spray, a minimum amount of electrolyte in the solvent is required, but this is so low that normal solvents contain enough electrolytes for this purpose. On the other hand, the maximum tolerable total concentration of electrolytes still to have a good sensitivity is about 10^{-3} M. Furthermore, volatile electrolytes are preferred to avoid

contamination of the source. With most samples, the problem is more to remove the salts rather than to add some. Also, sample dilution is often performed. Often HPLC methods have to be modified for ESI when they use high concentrations of buffers.

When it is believed that it could be better to add an electrolyte to improve sample detection, one should think about the electrochemical process when selecting it. We have seen, for instance, that adding an acid can improve the detection of negative ions. But the ESI process is not simple, and many trials are often needed.

1.12 Atmospheric Pressure Chemical Ionization

APCI is an ionization technique which uses gas-phase ion–molecule reactions at atmospheric pressure [76, 77]. It is a method analogous to CI (commonly used in GC–MS) where primary ions are produced by corona discharges on a solvent spray. APCI is mainly applied to polar and relatively non-polar compounds with moderate molecular weight up to about 1500 Da and gives generally monocharged ions. The principle governing an APCI source is shown in Figure 1.32.

The analyte in solution from a direct inlet probe or a liquid chromatography eluate at a flow rate between 0.2 and 2 ml min^{-1}, is directly introduced into a pneumatic nebulizer where it is converted into a thin fog by a high-speed nitrogen beam. Droplets are then displaced by the gas flow through a heated quartz tube called a desolvation/vaporization chamber. The heat transferred to the spray droplets allows the vaporization of the mobile phase and of the sample in the gas flow. The temperature of this chamber is controlled, which makes the vaporization conditions independent of the flow and from the nature of the mobile phase. The hot gas (120°C) and the compounds leave this tube. After desolvation, they are carried along a corona discharge electrode where ionization occurs. The ionization processes in APCI are equivalent to the processes that take place in CI but all of these occur under atmospheric pressure. In the positive ion mode, either proton transfer or adduction of reactant gas ions can occur to produce the ions of molecular species, depending on the relative proton affinities of the reactant ions and the gaseous analyte molecules. In the negative mode, the ions of the molecular species are produced by either proton abstraction or adduct formation.
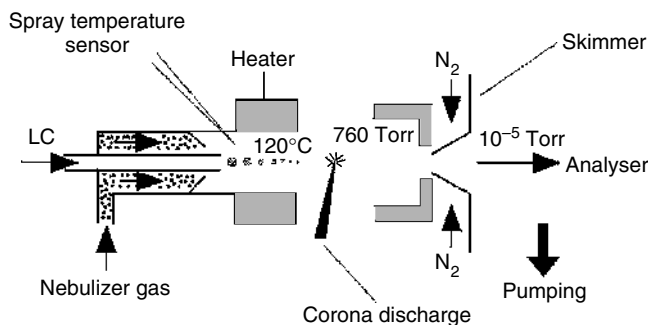
Figure 1.32
Diagram of an APCI source.

Generally, the evaporated mobile phase acts as the ionizing gas and reactant ions are produced from the effect of a corona discharge on the nebulized solvent. Typically, the corona discharge forms by electron ionization primary ions such as $N_2^{\bullet+}$ or $O_2^{\bullet+}$. Then, these ions collide with vaporized solvent molecules to form secondary reactant gas ions.

The electrons needed for the primary ionization are not produced by a heated filament, as the pressure in that part of the interface is atmospheric pressure and the filament would burn, but rather using corona discharges or β^- particle emitters. These two electron sources are fairly insensitive to the presence of corrosive or oxidizing gases.

As the ionization of the substrate occurs at atmospheric pressure and thus with a high collision frequency, it is very efficient. Furthermore the high frequency of collisions serves to thermalize the reactant species. In the same way, the rapid desolvation and vaporization of the droplets reduce considerably the thermal decomposition of the analyte. The result is production predominantly of ions of the molecular species with few fragmentations.

The ions produced at atmospheric pressure enter the mass spectrometer through a tiny inlet, or through a heated capillary, and are then focused towards the analyser. This inlet must be sufficiently wide to allow the entry of as many ions as possible while keeping a correct vacuum within the instrument so as to allow the analysis. The most common solution to all these constraints consists of using the differential pumping technique on one or several stages, each one separated from the others by skimmers [78]. In the intermediate-pressure region, an effective declustering of the formed ions occurs.

APCI has become a popular ionization source for applications of coupled HPLC–MS. Figure 1.33 shows an example of an application of HPLC–APCI coupling [79]. It shows the analysis obtained from extracts of maize plants. Six compounds are identified by mass spectrometry. These compounds have been identified as glucoconjugated DIMBOA (2,4-dihydroxy-7-methoxy-1,4-benzoxazin-3-one) and similar molecules that differ by the number of methoxy groups in the benzene ring and/or by the N-O methylation of the hydroxamate function. This example clearly shows the influence of the analyte on the type of observed molecular species. Indeed, the presence of an acidic group in the compound from peak 1 allows mainly the detection of deprotonated molecular ions, whereas the compound from peak 4 does not contain an acid group and thus leads only to the formation of adduct ions.

1.13 Atmospheric Pressure Photoionization

The APPI source is one of the last arrivals of atmospheric pressure sources [80, 81]. The principle is to use photons to ionize gas-phase molecules. The scheme of an APPI source is shown in Figure 1.34. The sample in solution is vaporized by a heated nebulizer similar to the one used in APCI. After vaporization, the analyte interacts with photons emitted by a discharge lamp. These photons induce a series of gas-phase reactions that lead to the ionization of the sample molecules. The APPI source is thus a modified APCI source. The main difference is the use of a discharge lamp emitting photons rather than the corona discharge needle emitting electrons. Several APPI sources have been developed since 2005 and are commercially available. The interest in the photoionization is that it has the potential to ionize compounds that are not ionizable by APCI and ESI, and in particular, compounds that are non-polar.
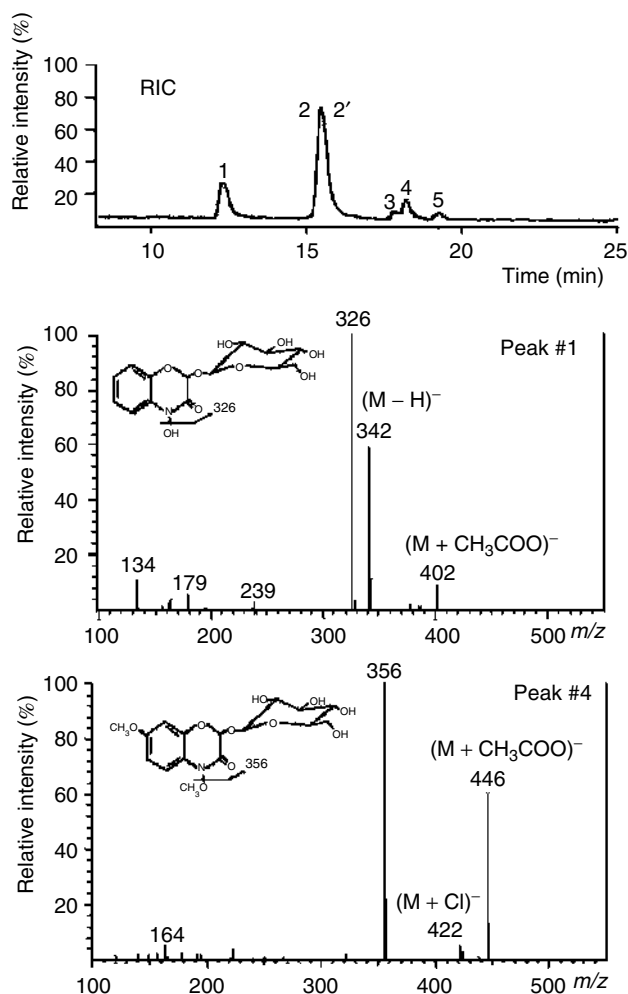
Figure 1.33
HPLC-APCI analysis of a mixture of glucoconjugated compounds related to DIMBOA. Spectrum from peak 4 does not display the deprotonated molecular species. The molecular mass (387 Da) is deduced from the adducts. The sample is obtained from extracts of maize plants. Reproduced (modified) from Cambier V., Hance T., and de Hoffmann E., Phytochem. Anal., 10, 119–126, 1999.

UV lamps generally employed provide photons at higher energy than the ionization potentials of the analytes but lower than those of the atmospheric gas and of the used solvents. This allows ions from the analytes to be selectively produced without ionizing the solvent, thus considerably reducing the background noise. As suggested by the data in Figure 1.35, the best lamp is the krypton discharge lamp emitting photons

Analyte
in solution

Nebulizer

Nebulizer gas

Desolvation/vaporization chamber

Heater

Heated capillary

N_2

UV lamp

hν

analyser

N_2
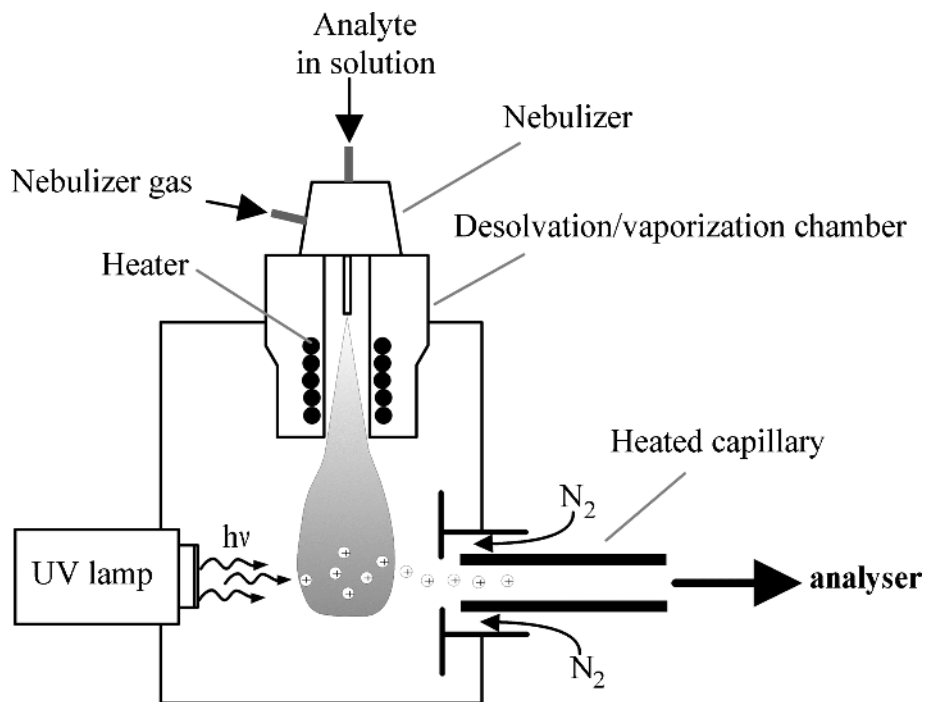
Figure 1.34
Scheme of an APPI source. The sample in solution is introduced perpendicular to the axis
of the analyser. The lamp is located in front of the entrance hole of the analyser. This
source has been designed initially for direct APPI (see text).

Lamps

Xe
8,4 eV

Kr
10,0 eV

Ar
11,2 eV

Analytes
7 eV - 10 eV

5   10   15

Ionization energy (IE)

Dopants   toluene   acetone
8,83 eV   9,70 eV

Solvents   methanol   acetonitrile   water
10,84 eV   12,20 eV   12,62 eV

Air   oxygen   nitrogen
12,07 eV   15,58 eV
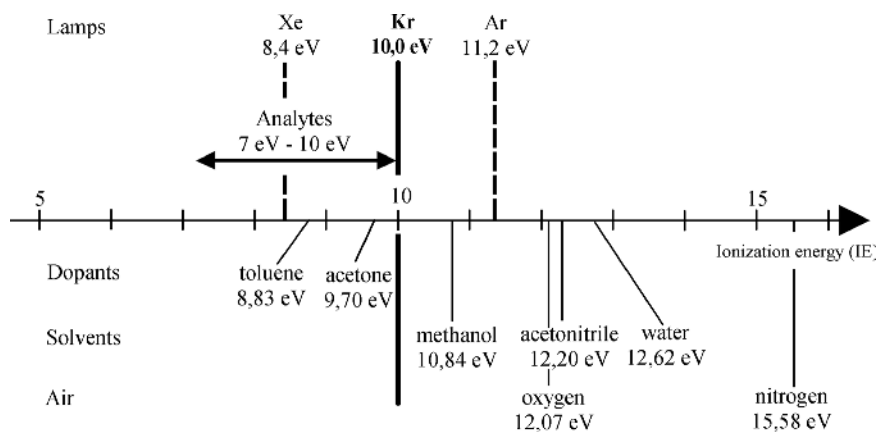
Figure 1.35
Ionization energy of molecules frequently present in APPI sources (solvents, doping
compounds, air components).

at 10.0 and 10.6 eV. Indeed, most analytes have ionization energies between 7 and 10 eV. On the other hand, air components (nitrogen and oxygen) and most of the common solvents (methanol, water, acetonitrile, etc.) have higher ionization potentials.

However, the direct ionization of the analyte is generally characterized by a weak efficiency. This can be partially explained by the solvent property to absorb photons producing photoexcitation without ionization. This reduces the number of photons available for the direct ionization of the sample, thus reducing the ionization efficiency. Consequently, ionization using doping molecules has also been described. It has indeed been shown that dopant at relatively high concentrations in comparison with the sample allows generally an increase in the efficiency of ionization from 10 to 100 times. This indicates that the process is initiated by the photoionization of the dopant. The dopant must be photoionizable and able to act as intermediates to ionize the sample molecules. The most commonly used dopants are toluene and acetone. Thus, two distinct APPI sources have been described: direct APPI and dopant APPI.

The mass spectra obtained by the APPI source in the positive ion mode are characterized by the presence of two main types of ions of the molecular species that may coexist [82]: the radical cation $M^{\bullet+}$ and the protonated molecule $[M + H]^+$. In direct APPI, the reaction is the classical photoionization leading to the radical cation of the molecular species:

$$M + h\nu \longrightarrow M^{\bullet+} + e^-$$
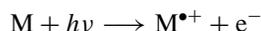
However, the often dominant presence of the protonated molecule suggests gas-phase ion–molecule reactions after the photoionization. The most likely reaction is the abstraction by the molecular ion of an hydrogen atom from a solvent molecule [83]:

$$M^{\bullet+} + S \longrightarrow [M + H]^+ + (S - H)^\bullet$$

In the presence of a dopant in the positive ion mode, the first step of the ionization process is the production of a radical ion from the dopant molecule by direct photoionization:

$$D + h\nu \longrightarrow D^{\bullet+} + e^-$$
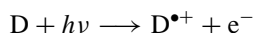
This radical cation may then ionize a solvent molecule by proton transfer, if the proton affinity of the solvent molecule is higher than that of the deprotonated radical cation. It seems that the solvent acts as aggregates, having then a higher proton affinity. These protonated solvent molecules may then ionize analyte molecules by proton transfer if these last have a higher proton affinity than the solvent molecules:

$$D^{\bullet+} + S \longrightarrow [S + H]^+ + (D - H)^\bullet$$
$$M + [S + H]^+ \longrightarrow [M + H]^+ + S$$

Alternatively, if the ionization energy of the analyte is lower than that of the dopant, the radical cation of the dopant can directly interact with an analyte molecule and ionization by charge exchange of the analyte can occur to produce the molecular radical cation of the analyte:

$$D^{\bullet+} + M \longrightarrow M^{\bullet+} + D$$

Thus, besides the direct photoionization, the analytes in positive APPI mode are ionized either by charge exchange or by proton transfer. The direct ionization and the charge exchange processes allow the ionization of non-polar compounds. This is not possible either with APCI or ESI.

The formation of either the radical cation $M^{\bullet+}$ or the protonated $[M+H]^+$ molecule, or both together, will depend on the relative ionization energies or proton affinities of the sample molecules and the solvent components. Concerning the solvent, the charge exchange is favoured for solvents with low proton affinity (water, chloroform, cyclohexane, etc.), while solvents with higher proton affinities (methanol, acetonitrile, etc.) will favour proton transfer.

APPI is also efficient in negative ion mode, in so far as a dopant is used [84]. Indeed, in this ionization mode, analysis made without dopant dramatically decreases the sensitivity. All the reactions leading to the ionization of the analytes are initiated by thermal electrons produced with the photoionization of the dopant. Hence, solvents of high positive electron affinity, for example halogenated solvents, inhibit the ionization of all the analytes because these solvents capture all the available thermal electrons in the source.

Production of the negative molecular ion $M^{\bullet-}$ by electron capture is possible for any analyte presenting a positive electron affinity:

$$M + e^- \longrightarrow M^{\bullet-}$$
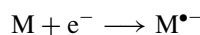
This molecular radical anion can also be produced by charge exchange reaction with $O_2^{\bullet-}$, itself produced in the source by electron capture of an oxygen molecule from the atmosphere. In this case, the electron affinity of the analyte must be higher than 0.45 eV, this value corresponding to the electron affinity of the O_2 molecule:

$$O_2 + e^- \longrightarrow O_2^{\bullet-}$$

$$M + O_2^{\bullet-} \longrightarrow M^{\bullet-} + O_2$$
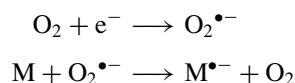
Formation of the deprotonated molecular ion is also possible for analytes with high gas-phase acidity. This is due to the presence in the source of basic species often produced from the solvent. Solvent evaporated in the source acts as the ionization gas in chemical ionization, yielding species that can react with the analyte by proton transfer. This reaction is, however, only possible if the acidity of the analyte is higher than that of the solvent:

$$M + [S - H]^- \longrightarrow [M - H]^- + S$$

Besides the solvent, other species may participate in the proton abstraction from the analyte molecules. For instance, $O_2^{\bullet-}$ has a strong basicity in the gas phase and may react with other molecules from the solvent or the analyte by proton transfer. These molecules must have acidity lower than $1451 \, \text{kJ} \, \text{mol}^{-1}$, this value corresponding to the gas-phase acidity of the $HO_2^{\bullet}$ species:

$$S + O_2^{\bullet-} \longrightarrow [S - H]^- + HO_2^{\bullet}$$

$$M + O_2^{\bullet-} \longrightarrow [M - H]^- + HO_2^{\bullet}$$
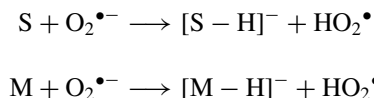
Ionization of analytes by proton abstraction is suppressed if the solvent molecules have higher gas-phase acidities than the analytes, because then transfer of the proton occurs in the opposite way, from the solvent to the analyte. In the same way, the presence of compounds of high gas-phase acidity from the solvent or other additives will suppress the

ionization of the analyte, even if they have a positive electronic affinity. This is probably due to the neutralization by proton transfer of the $O_2^{\bullet-}$ ions, leading to the inhibition of all charge exchange reactions.

Thus, the negative APPI mode will produce molecular ions from the analytes by charge exchange or by electron capture if they have a sufficient electron affinity. Analytes that have high gas-phase acidity will be mainly ionized by proton transfer to yield deprotonated molecular ions.

Compared with APCI, APPI is more sensitive to the experimental conditions. Properties of solvents, additives, dopants or buffer components can strongly influence the selectivity or sensitivity of the detection of analytes. Nevertheless, this technique allows the ionization of compounds not detectable in APCI or ESI, mainly non-polar compounds. For these last compounds, APPI is a valuable alternative. Thus, APPI is a complementary technique to APCI and ESI. However, for a given substance it remains difficult to predict which ionization source (APPI, APCI or ESI) will give the best results. Only preliminary tests will allow the choice of the best ionization source. APPI appears to be efficient for some compound classes such as flavonoids, steroids, drugs and their metabolites, pesticides, polyaromatic hydrocarbons, etc. [85].

1.14 Atmospheric Pressure Secondary Ion Mass Spectrometry

Some ionization methods have been developed in the last few years that allow a sample at atmospheric pressure and at ground potential to be directly exposed to an ionizing beam. Some of them allow the exposure of living material, for example a finger.

1.14.1 Desorption Electrospray Ionization

A new ionization method called desorption electrospray ionization (DESI) was described by Cooks and his co-workers in 2004 [86]. This direct probe exposure method based on ESI can be used on samples under ambient conditions with no preparation. The principle is illustrated in Figure 1.36. An ionized stream of solvent that is produced by an ESI source is sprayed on the surface of the analysed sample. The exact mechanism is not yet established, but it seems that the charged droplets and ions of solvent desorb and extract some sample material and bounce to the inlet capillary of an atmospheric pressure interface of a mass spectrometer. The fact is that samples of peptides or proteins produce multiply charged ions, strongly suggesting dissolution of the analyte in the charged droplet. Furthermore, the solution that is sprayed can be selected to optimize the signal or selectively to ionize particular compounds.

The sample may be exposed as such or deposited on a sample holder that may be made of any material, conducting or non-conducting, provided it does not produce background noise. Furthermore, the sample can be freely moved or manipulated during the experiment. An interesting feature is that reactants can be introduced in the spray solution to react with the sample. Another interesting feature of DESI is the ability to map the position of analytes of the native surfaces, such as plant or animal tissues. It has also been demonstrated that DESI can be used with thin-layer chromatography [87].
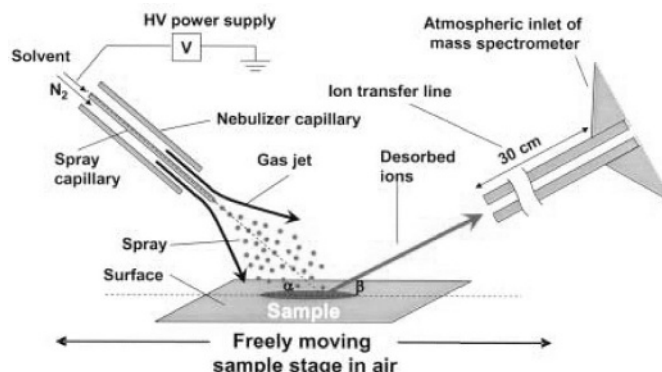
Figure 1.36
A pneumatically assisted ion spray source is oriented at 45° to-
wards a sample. The nitrogen spray is adjusted so as to have
a linear speed of the droplets of about 35 m s^{-1}. From Takats
Z., Wiseman J.M., Gologan B. and Cooks R.G., Science, 306,
471–473, 2004. Reprinted, with permission.

A broad range of compounds, including small non-polar molecules or large polar
molecules like peptides and proteins, have been analysed successfully by DESI. This
method can also detect drug molecules on the surface of the skin. As an example, Figure
1.37 shows the spectrum obtained by exposing the finger of a person after intake of 10 mg
of the antihistaminic Loratadine. This drug is characterized by a protonated molecular ion
at *m/z* 383 with the isotopic distribution at *m/z* 383/385 due to one chlorine atom. Other
applications include explosives on tanned porcine leather, sections of stems or seeds from
vegetals, and so on. The resulting mass spectra are similar to normal ESI mass spectra.
They show mainly singly or multiply charged molecular ions from small or large analytes,
respectively.

1.14.2 Direct Analysis in Real Time

The direct analysis in real time (DART) method has been described by Cody *et al.* [88] and
commercialized by JEOL. This method allows direct detection of chemicals on surfaces,
in liquids and in gases without the need for sample preparation. All of these analyses take
place under ambient conditions in a space just in front of the inlet of the mass spectrometer.
The sample is not altered because no exposure to high voltage or to vacuum is required.

In the source, a gas such as helium or nitrogen is introduced and submitted to a beam of
electrons by applying a high-voltage potential between two electrodes as shown in Figure
1.38. Ions, electrons and neutral species with electronic or vibronic excitation are produced.
This resulting plasma passes through a series of electrodes designed to remove any charged
species, leaving only neutral species that then interact with the sample and the atmosphere.
It seems that mainly these excited neutral species produce the ionization of the sample
molecules.

Several mechanisms involved in ion formation are possible, depending on the analysed
molecule and the operating conditions like the polarity and the gas used. In positive ion
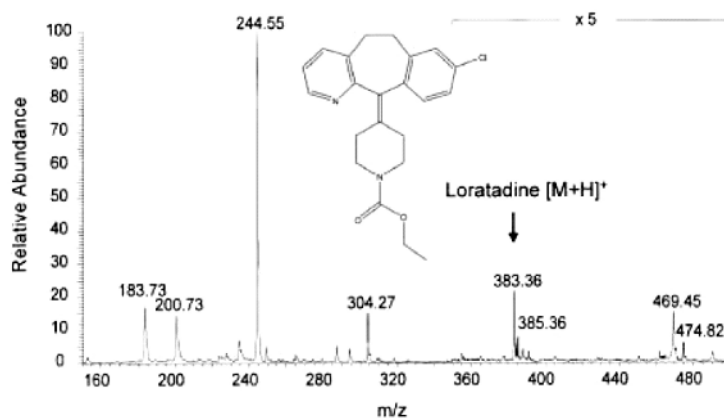
Figure 1.37
Spectrum obtained by DESI exposure of the finger of a person after intake of 10 mg Loratadine. From Takats Z., Wiseman J.M., Gologan B. and Cooks R.G., Science, 306, 471–473, 2004. Reprinted, with permission.
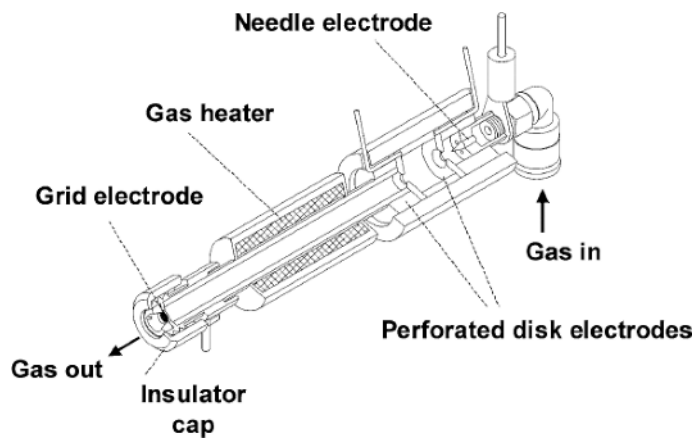
Figure 1.38
Cutaway view of a DART source. Discharge is produced in the first chamber and the gas then flows into a second chamber where the ions can be discharged. The gas flows through a tube that can optionally be heated and then flows out to the sample through a grid that allows removal of ions of opposite polarity. From Cody R.B., Laramee J.A. and Dupont Durst H., Anal. Chem., 77, 2297–2302, 2005. Reprinted, with permission.
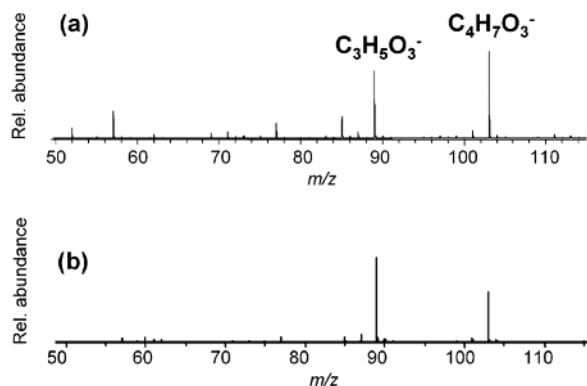
Figure 1.39
Detection of γ-hydroxybutyrate (a) in gin at 10 ppm
and (b) as sodium salt on the rim of a drinking glass.
From Cody R.B., Laramee J.A. and Dupont Durst H.,
Anal. Chem., 77, 2297–2302, 2005. Reprinted, with
permission.

mode, the simplest process is Penning ionization involving transfer of energy from the
excited gas to an analyte, leading to the radical cation of the molecular species:

$$G^* + M \longrightarrow M^{\bullet+} + G + e^-$$

Another ionization process that is the main process when helium is used as the gas is proton
transfer. This type of ionization occurs when metastable helium atoms react with water in
the atmosphere to produce ionized water clusters that can protonate the sample molecule,
leading to the protonated molecule.

   Negative ions can be formed by electron capture due to the presence of thermalized
electrons produced by Penning ionization or by surface Penning ionization. Negative ions
can also be obtained by reactions of analyte molecules with negative ions formed from
atmospheric water and oxygen to produce the deprotonated molecule.

   The mechanism involved in desorption of materials from surfaces by this method is
not well understood. One of these mechanisms is the thermal desorption because heating
the gas helps desorption of some analytes. However, the successful analysis by DART
of analytes having little or no vapour pressure indicates that other processes occur. The
transfer of energy to the surface by metastable atoms and molecules has been proposed as
the mechanism to facilitate desorption and ionization of these analytes.

   Hundreds of compounds on different surfaces have been tested, many examples con-
cerning mainly explosives on different surfaces, as well as the analysis of a urine sample
containing the drug ranitidine and the analysis of capsaicin in different parts of a pepper
pod. Detection of γ-hydroxybutirate, an illegal drug classified as a sedative–hypnotic, is
shown in Figure 1.39.

   DART produces relatively simple mass spectra characterized by the presence of two main
types of ions of the molecular species: $M^{\bullet+}$ or $[M+H]^+$ in positive ion mode and $M^{\bullet-}$
or $[M-H]^-$ in negative ion mode. Fragmentation is observed for most of the compounds.
These results appear similar to those obtained with DESI, but no multiply charged ions are

produced. Consequently, the range of analytes that can be analysed by DART is less broad than by DESI. Furthermore, DART cannot be used for the spatial analysis of surfaces.

1.15 Inorganic Ionization Sources

Mass spectrometry is not only an indispensable tool in organic and biochemical analysis, but also a powerful technique for inorganic analysis [89–91]. Indeed, over the last 20 years the application of mass spectrometry to inorganic and organometallic compounds has revolutionized the analysis of these compounds. Important advances have been made in the diversification of ionization sources, in the commercial availability of the instruments and in the fields of applications.

Mass spectrometry is now widely used for inorganic characterization and microsurface analysis. EI is the preferred ionization source for volatile inorganic compounds, whereas the others which are non-volatile may be analysed using ionization sources already described such as SIMS, FD, FAB, LD or ESI [92–94]. The example in Figure 1.40 shows the analysis of orthorhombic sulfur (S_8 ring) and $Cr(CO)_2(dpe)_2$, respectively obtained with an EI source and an ESI source.

In addition, quantitative and qualitative elemental analysis of inorganic compounds with high accuracy and high sensitivity can be effected by mass spectrometry. For elemental analysis, atomization of the analysed sample that corresponds to the transformation of solid matter in atomic vapour and ionization of these atoms occur in the source. These atoms are then sorted and counted with the help of mass spectrometry. The complete decomposition of the sample in the ionization source into its constituent atoms is necessary because incomplete decomposition results in complex mass spectra in which isobaric overlap might cause unsuspected spectral interferences. Furthermore, the distribution of any element in different species leads to a decrease in sensitivity for this element.

Four techniques based on mass spectrometry are widely used for multi-elemental trace analysis of inorganic compounds in a wide range of sample types. These techniques are thermal ionization (TI), spark source (SS), glow discharge (GD) and inductively coupled plasma (ICP) mass spectrometry. In these techniques, atomization and ionization of the analysed sample are accomplished by volatilization from a heated surface, attack by electrical discharge, rare-gas ion sputtering and vaporization in a hot flame produced by inductive coupling.

All of these ionization sources are classical sources used also in optical spectroscopy. The only fundamental difference is that these sources are not used for atomization/excitation processes to generate photons but to generate ions.

1.15.1 Thermal Ionization Source

Thermal ionization is based on the production of atomic or molecular ions at the hot surface of a metal filament [95, 96]. In this ionization source, the sample is deposited on a metal filament (W, Pt or Re) and an electric current is used to heat the metal to a high temperature. The ions are formed by electron transfer from the atom to the filament for positive species or from the filament to the atom for negative species. The analysed sample can be fixed to the filament by depositing drops of the sample solution on the filament surface followed by evaporation of the solvent to complete dryness, or by using electrodeposition methods.
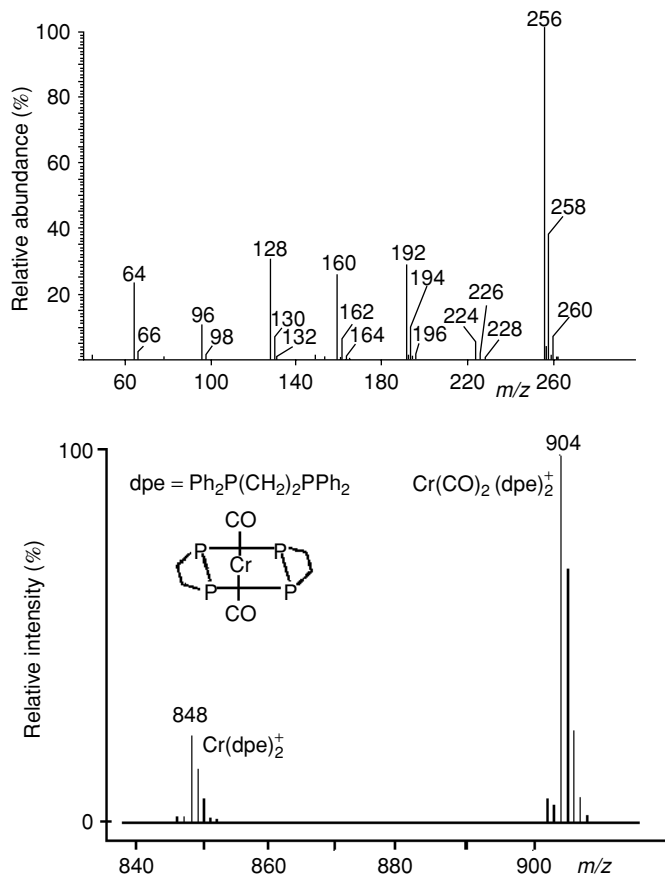
Figure 1.40
Analysis of inorganic compounds by mass spectrometry. Top: EI
spectrum of orthorhombic sulfur (S_8). Bottom: ESI spectrum of
$Cr(CO)_2(dpe)_2$. The last spectrum is redrawn from data taken
from Traeger J.C. and Colton R., Adv. Mass Spectrom., 14, 637–
659, 1998.

Single, double and triple filaments have been broadly used in thermal ionization sources.
In a single filament source, the evaporation and ionization process of the sample are
carried out on the same filament surface. Using a double filament source, the sample is
placed on one filament used for the evaporation while the second filament is left free
for ionization. In this way, it is possible to set the sample evaporation rate and ionization
temperature independently, thus separating the evaporation from the ionization process. This
is interesting when the vapour pressure of the studied elements reaches high values before
a suitable ionization temperature can be achieved. A triple filament source can be useful to
obtain a direct comparison of two different samples under the same source conditions.

Positive and negative ions can be obtained by the thermal ionization source. High yields
of positive and negative ions are obtained for atoms or molecules with low ionization
potential and with high electron affinity, respectively. Owing to the ionization process and
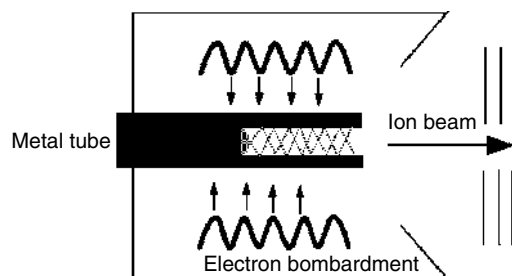
Figure 1.41
Schematic representation of a thermal ionization
cavity source.

their physical parameters, metals can be analysed in positive ion mode, whereas many
non-metals, semimetals and transition metals or their oxides are able to form negative
thermal ions.

In thermal ionization sources, the most abundant ions are usually the singly charged
atomic ions. No multiply charged ions can be observed under normal ionization conditions.
Cluster ions occur very seldom. However, some metal compounds lead to abundant metal
oxide ions.

For thermal ionization filament sources, the ionization efficiency varies from less than
1 % to more than 10 %, depending on the analysed elements. A significant improvement
of ionization efficiency can be observed with the use of a thermal ionization cavity (TIC)
source [97]. In this type of thermal source, as schematically displayed in Figure 1.41, a
refractory metal tube is used instead of a filament to evaporate and ionize the sample. High
ionization temperatures are achieved by using high-energy electron bombardment to heat
the tube. As the sample evaporates, the gaseous atoms interact with each other and with
the inner wall of the cavity to produce ions. Compared with filament sources, the cavity
sources can provide orders-of-magnitude enhancement of the ionization efficiency.

1.15.2 Spark Source

In spark sources, electrical discharges are used to desorb and ionize the analytes from
solid samples [98]. As shown in Figure 1.42, this source consists of a vacuum chamber
in which two electrodes are mounted. A pulsed 1 MHz radio-frequency (RF) voltage of
several kilovolts is applied in short pulses across a small gap between these two electrodes
and produces electrical discharges. If the sample is a metal it can serve as one of the two
electrodes, otherwise it can be mixed with graphite and placed in a cup-shaped electrode.

Atomization is accomplished by direct heating of the electrode by the electron component
of the discharge current and by the discharge plasma. Then, ionization of these atoms which
occurs in the plasma is due mainly to plasma heating by electrons accelerated by the electric
field. Chemical reactions can also take place in the plasma, leading to the formation of
clusters.

Various types of positive ions are produced in a spark discharge such as singly and
multiply charged atomic ions, polymer ions and heterogeneous compound ions. A spark
source mass spectrum is always characterized by singly and multiply charged ions of the
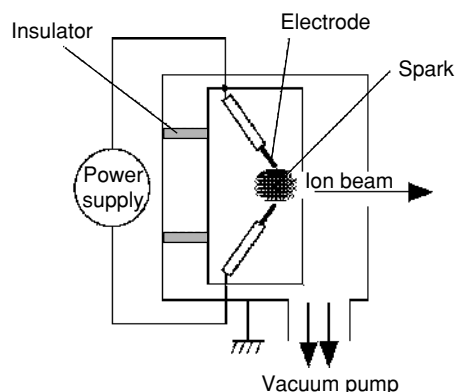
Figure 1.42
Typical spark ion source.

major constituents, with a decrease of their intensities when their charges increase. Also, the singly charged species are always the most intense for minor constituents and are usually the only ones used for analytical purposes. Another abundant class of ions detected in a spark source is heterogeneous compounds ions formed by the association of the matrix with hydrogen, carbon, nitrogen and oxygen.

It must be noted that this technique does not provide accurate quantitative analysis.

1.15.3 Glow Discharge Source

A glow discharge (GD) source is particularly effective at sputtering and ionizing compounds from solid surfaces [99–101]. This source is indicated schematically in Figure 1.43. A glow discharge source consists of one cathode and one anode in a low-pressure gas (0.1–10 Torr), usually one of the noble gases. Argon is the most commonly used gas because of its low cost and its high sputtering efficiency. The sample is introduced in this source as the cathode. Application of an electric current across the electrodes causes breakdown of the gas and the acceleration of electrons and positive ions towards the oppositely charged electrodes. Argon ions from the resulting plasma attack by bombardment the analyte at the surface of the cathode. Collisions of these energetic particles on the surface transfer their kinetic energy. The species near the surface can receive sufficient energy to overcome the lattice binding and be ejected mainly as neutral atoms. The sample atoms liberated are then carried into the negative glow region of the discharge where they are ionized mainly by electron impact and Penning ionization (Figure 1.43).

A simple DC power supply at voltages of 500–1000 V and currents of 1–5 mA suffices to obtain glow discharge. However, pulsed DC discharges allow use of higher peak voltages and currents, whereas an RF discharge allows the analysis of poorly conducting samples directly.

The principal application of glow discharge is in bulk metal analysis. The conducting solid samples can be made into an electrode whereas non-conducting materials are compacted with graphite into the electrode for analysis. Solution samples can also be analysed by drying the sample on a graphite electrode. Other applications such as the examination of thin films or solution residues are also possible. Glow discharge ion sources can also be
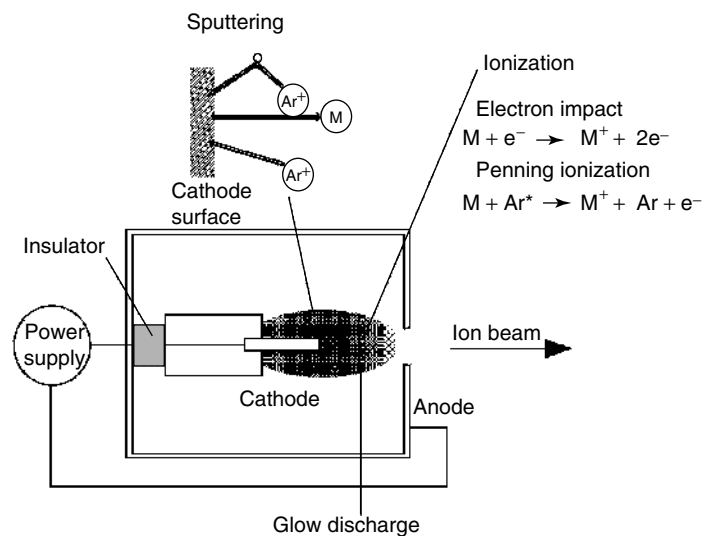
Figure 1.43
Schematic diagram of a glow discharge source with sputtering at the
cathode surface and ionization in the discharge.

used in conjunction with laser ablation. The pulse of ablated material enters directly into
the plasma of the glow discharge where it undergoes ionization.

Owing to the ionization process, only positive ions can be obtained by the glow discharge
ionization source. Consequently, the spectra obtained with the glow discharge source are
characterized by singly charged positive ions of the sputtered cathode atoms. Almost no
doubly charged ions from the sample are observed. Some diatomic cluster ions are formed
but are normally observed only for major constituents. The noble gas used (usually Ar) and
residual gases such as nitrogen, oxygen and water vapor are always observed.

Only a low net ionization in the discharge is produced. The ionization efficiency is
estimated to be 1 % or less. However, glow discharge produces an atomic vapour represen-
tative of the cathode constituents and the discharge ionization processes are also relatively
non-selective. Also, because most elements are sputtered and ionized with almost the same
efficiency in the source, quantitative analysis without a standard is possible.

It must be noted that glow discharge requires several minutes for the extracted ions to
reach equilibrium with elemental concentrations in the analysed sample. Thus, the sample
throughput with this technique is relatively low.

1.15.4 Inductively Coupled Plasma Source

An inductively coupled plasma source is made up of a hot flame produced by inductive
coupling in which a solution of the sample is introduced as a spray [102–104]. This
source consists of three concentric quartz tubes through which streams of argon flow.
As shown in Figure 1.44, a cooled induction coil surrounds the top of the largest tube.
This coil is powered by an RF generator that produces between 1.5 and 2.5 kW at 27 or
40 MHz typically. The gas at atmospheric pressure that sustains the plasma is initially made
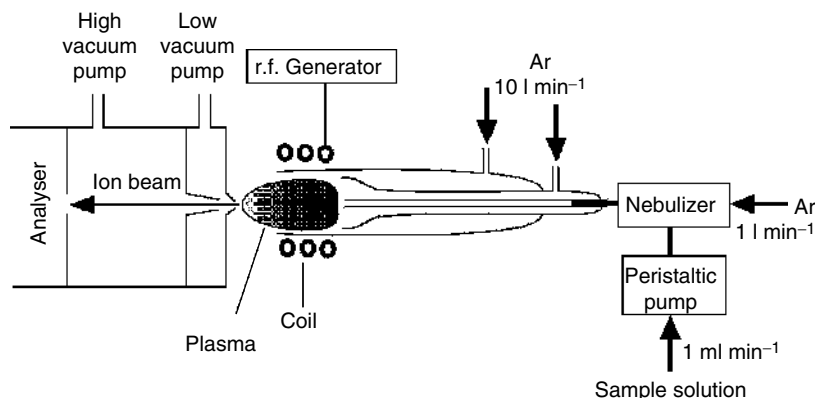
Figure 1.44
Schematic diagram of an inductively coupled plasma source.

electrically conductive by Tesla sparks which lead to the ionization of the flowing argon. Then, the resulting ions and the produced electrons which are present in the discharge interact with the high-frequency oscillating inductive field created by the RF current in the coil. They are consequently accelerated, collide with argon atoms and ionize them. The released products by this ionization then undergo the same events until the argon ionization process is balanced by the opposing process corresponding to ion–electron recombination. These colliding species cause heating of the plasma to a temperature of about $10\,000\,K$. This temperature requires thermal isolation from the outer quartz tubes by introducing a high-velocity flow of argon of about $10\,l\,min^{-1}$ tangentially along the walls of these tubes.

The sample is carried into the hot plasma as a thermally generated vapour or a finely divided aerosol of droplets or microparticulates by argon flowing at about $1\,l\,min^{-1}$ through the central tube. The high temperatures rapidly desolvate, vaporize and largely atomize the sample. Furthermore, this plasma at high temperature and at atmospheric pressure is a very efficient excitation source. The resulting atoms may spend several milliseconds in a region at a temperature between 5000 and $10\,000\,K$. Under these conditions, most elements are ionized to singly charged positive ions with an ionization efficiency close to $100\,\%$. Some elements can be ionized to higher charged states but with very low abundance. Ions are extracted from the plasma and introduced in the mass analyser through a two-stage vacuum-pumped interface containing two cooled metal skimmers.

The most common introduction of the samples in this source consists of a pneumatic nebulizer which is driven by the same flow of argon which carries the resulting droplets in the plasma. An ultrasonic nebulizer and heated desolvation tube are also used because they allow a better droplet size distribution which increases the load of sample into the plasma. Generally, the sample solutions are continuously introduced in the nebulizer at the rate of about $1\,ml\,min^{-1}$ with the help of a peristaltic pump. However, this is not acceptable with small-sample solutions. Therefore an alternative method using the flow injection technique is employed to introduce a small sample of about $100\,\mu l$. The sample solution is injected into a reference blank flow so that the sample is transported in the nebulizer and a transitory signal is observed.

Other alternative methods of sample introduction have been applied. A very small volume of liquid ($<10\,\mu l$) or solid sample may be introduced in the plasma as a vapour produced

1 H																	2 He
3 * Li	4 * Be											5 * B	6 • C	7 N	8 O	9 — F	10 Ne
11** Na	12 * Mg											13 * Al	14 • Si	15 — P	16 — S	17 — Cl	18 Ar
19 — K	20 • Ca	21** Sc	22** Ti	23** V	24** Cr	25** Mn	26•• Fe	27** Co	28** Ni	29** Cu	30** Zn	31** Ga	32** Ge	33•• As	34•• Se	35 • Br	36 Kr
37** Rb	38** Sr	39** Y	40** Zr	41** Nb	42** Mo	43** Tc	44** Ru	45** Rh	46** Pd	47** Ag	48** Cd	49** In	50** Sn	51** Sb	52** Te	53** I	54 Xe
55** Cs	56** Ba	57** La	72** Hf	73** Ta	74** W	75** Re	76** Os	77** Ir	78** Pt	79 Au	80 Hg	81** Ti	82** Pb	83** Bi	84 Po	85 At	86 Rn
87 Fr	88 Ra	89 Ac															

58** Ce	59** Pr	60** Nd	61 Pm	62** Sm	63** Eu	64** Gd	65** Tb	66** Dy	67** Ho	68** Er	69** Tm	70** Yb	71** Lu
90** Th	91 Pa	92** U	93 Np	94 Pu	95 Am	96 Cm	97 Bk	98 Cf	99 Es	100 Fm	101 Md	102 No	103 Lr

**	$0.001-0.01\ \mu g\ l^{-1}$	••	$0.1-1\ \mu g\ l^{-1}$	—	$>10\ \mu g\ l^{-1}$
*	$0.001-0.1\ \mu g\ l^{-1}$	•	$1-10\ \mu g\ l^{-1}$		No available data

Figure 1.45
Analytical sensitivity of the elements by ICP-MS.

by electrothermal vaporization (ETV), which vaporizes the sample by flash evaporation from a filament heated by a current pulse. In this case, the sample vapour is produced in a short time of a few seconds and is transferred to the plasma as a gas. Solid samples at atmospheric pressure can also be introduced by laser ablation. This technique also allows spatial analysis of the surface of a sample.

It must be noted that handling samples in solution allows automation and high sample throughput. Indeed, the sample throughput for an ICP-MS instrument is typically 20–30 elemental determinations in a few minutes, depending on such factors as the concentration levels and precision required. Handling solution samples includes other advantages such as the record and the subtraction of a true blank spectrum, the adjustment of the dynamic range by dilution, the simplicity of adding internal standards, etc.

1.15.5 Practical Considerations

When compared with optical spectrometric techniques of elemental analysis, the techniques based on mass spectrometry provide an increase in sensitivity and in analytical working range of some orders of magnitude. For instance, the detection limits with ICP-MS are three orders of magnitude better than ICP-optical emission spectrometry (ICP-OES). Figure 1.45 shows the maximum sensitivity obtained for the different elements, using an ICP-MS coupling with a quadrupole.

These techniques are relatively interference free but there are, nevertheless, two major types of interferences. A first type is the matrix interferences which induce suppression or enhancement of the analyte signal. Such interferences are due to identity and composition of the sample itself. As they cause differences between samples and standards for a particular

element concentration, they lead to quantitative errors. Matrix effects are generally more serious with these techniques than with optical spectrometric techniques.

However, the most common interferences are the spectral interferences, also called isobaric interferences. They are due to overlapping peaks which can mask the analyte of interest and can give erroneous results. Such interferences may occur from ions of other elements within the sample matrix, elemental combination, oxide formation, doubly charged ions, and so on.

A solution to the overlapping peaks problem consists of identifying the interfering species and applying corrections for their contribution to the signal from the analyte. Corrections are based on identifying an isotope of the suspected interfering element that does not itself suffer from spectral interference and that can be measured with a sufficiently accurate signal. Then, knowing the relative natural abundance of the isotopes, the contribution of this interfering element to the signal at the mass of interest can be calculated. This correction is not appropriate when the interference is many times more abundant than the analyte because the error on the measurement can be too large.

Another very straightforward solution to the overlapping peaks problem is to increase the resolution power of the mass spectrometer. High-resolution mass spectrometers have the ability to resolve many isobaric interferences from the analyte and thus allow unambiguous quantitative analysis to be carried out. However, it should be noted that the sensitivity decreases when the resolution increases.

1.16 Gas-Phase Ion–Molecule Reactions

While EI does not imply any ion–molecule reactions, the latter provide the whole basis of CI and of all the API methods. Other ionization methods give rise to ion–molecule reactions as secondary processes. We will now emphasize some characteristics of these gas-phase reactions and compare them with condensed-phase reactions.

Figure 1.46 displays the energy characteristics of both the gas-phase and aqueous solution phase for the substitution reaction [105]:

$$Cl^- + CH_3Br \longrightarrow CH_3Cl + Br^-$$

In the condensed phase, molecules and *a fortiori* ions are strongly solvated. This solvation cage must be at least partially destroyed in order to form the activated complex. This requires a lot of energy and high activation energies are thus observed. Furthermore, each species mingles with the surrounding molecules and continuously exchanges energy.

In the gas phase the opposite occurs: the naked ion interaction with the molecule is exothermic, which leads to the formation of an ion–molecule complex. Some activation energy thus becomes necessary in order to transform the $Cl^- \cdot CH_3Br$ complex into the activated complex and finally into $Br^- \cdot CH_3Cl$. As can be seen in Figure 1.46, this activation energy is generally lower than the energy produced by the first step. Thus, if compared with the starting reactants, the actual activation energy is negative. Another very important difference must be noted: the mass spectrometry literature refers to the gas phase but this association with conventional gases is incorrect. Indeed, the reacting species generally considered in mass spectrometry do not interact with each other, owing to the low pressure, and thus do not continuously exchange energy with surrounding molecules. They are never present as an equilibrium phase. Hence the energy produced by the association of the ion

Table 1.4 Rate constants for the reaction $CH_3Br + OH^- \rightleftharpoons CH_3OH + Br^-$ for naked and solvated ions in the gas phase and in aqueous solution.

Hydroxide ion	Rate constant ($cm^3\ mol^{-1}\ s^{-1}$)
OH^-	$(1.0 \pm 0.2) \times 10^{-9}$
$OH^- \cdot H_2O$	$(6.3 \pm 2.5) \times 10^{-10}$
$OH^- \cdot (H_2O)_2$	$(2 \pm 1) \times 10^{-12}$
$OH^- \cdot (H_2O)_3$	$<2 \times 10^{-13}$
Aq. sol. $OH^- \cdot (H_2O)_x$	2.3×10^{-25}
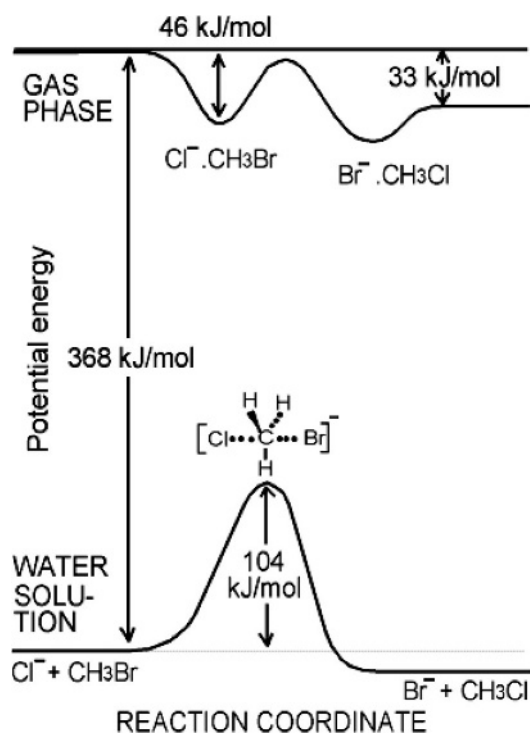
Figure 1.46
Potential energy diagram for a substitution reaction in the gas phase and in solution in water. Reproduced (modified), with permission from McIver R.T., Sci. Am., 243, 148, 1980.

with the molecule remains in the complex, thereby allowing it to overcome the activation barrier. Deactivation through radiation is a relatively slow process. This energy further allows the separation of the products into free the Br^- ion and CH_3Cl molecules.

Figure 1.47 displays the results obtained by measuring the kinetic and thermodynamic parameters for the following reaction [106]:

$$OH^- + CH_3Br \rightleftharpoons Br^- + CH_3OH$$
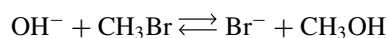
Table 1.5 Definition of most important gas-phase thermodynamic data.

Gas-phase basicity	Gas-phase acidity
$M + H^+ \rightleftharpoons MH^+$	$AH \rightleftharpoons A^- + H^+$
$PA = -\Delta H^\circ GB = -\Delta G^\circ$	ΔH°_{ACID} and ΔG°_{ACID}
Exothermic	Endothermic
Ionization energy (IE)	**Electron affinity (EA)**
$M \rightleftharpoons M^{\bullet+} + e^-$	$M + e^- \rightleftharpoons M^{\bullet-}$
$IE = \Delta H^\circ$	$EA = -\Delta H^\circ$
Endothermic	Exothermic or weakly endothermic

Note. The same values are available for radicals instead of molecules.

$$\overset{A}{OH^- + CH_3Br} \rightleftharpoons OH^-.CH_3Br \rightleftharpoons CH_3OH.Br^- \rightleftharpoons \overset{B}{CH_3OH + Br^-}$$
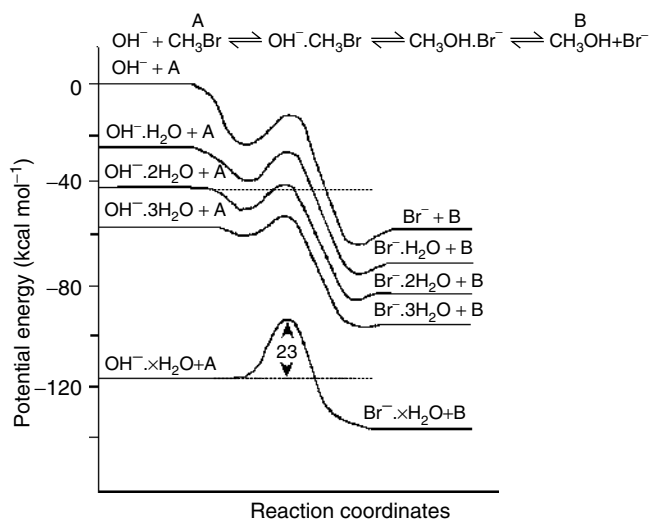
Figure 1.47
(A) CH_3Br; (B) CH_3OH. Potential energy profile for differently solvated ions reacting with molecules. Reproduced (modified), with permission from Bohme D.K. and Mackay G.I., J. Am. Chem. Soc., 103, 978, 1981.

In this case, the authors succeeded in measuring separately the reaction characteristics both for the naked OH^- ion and for the ion solvated by one to three water molecules. As the number of water molecules increases, the shape of the curves approaches that for the reaction in aqueous solution. The observed rate constants are given in Table 1.4. The rate constant for the gas-phase ion–molecule reaction is 10^{16} times greater than the rate observed in solution. This experimentally observed factor goes up to 10^{20} in the case of other reactions.

Let us now address another problem: are all the ion–molecule reactions possible?

The aim of this section is to give an overview of the factors determining the formation of the various types of ions encountered in the different ionization modes. Exceptions and examples are given in the sections dedicated to the ionization methods and to the fragmentations.

Table 1.6 Gas-phase basicities ($kJ\,mol^{-1}$) showing the influence of the protonated atoms and of the substituents. Note that the phenyl group is an electron donor in the gas phase.

$kJ\,mol^{-1}$	GB		GB		GB
NH_3	819	H_2O	660	H_2S	674
CH_3NH_2	864	CH_3OH	724	CH_3SH	742
$(C_2H_5)_2NH$	878	$(C_2H_5)_2O$	801	$(CH_3)_2S$	801
$PhNH_2$	851	$PhOH$	786	CH_3CHO	736
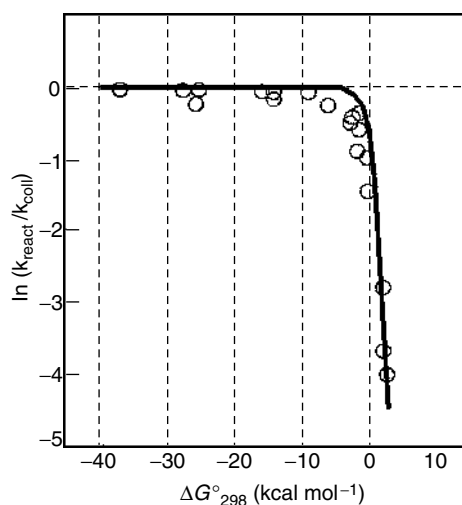
Figure 1.48
The natural logarithm of the number of reactions per collision ratio indicates that the proton transfer is almost 100 % efficient when the process is exergonic. When it becomes endergonic, the efficiency drops sharply. Reproduced (modified), with permission from Bohme D., Mackay G.I. and Schiff H.I., J. Chem. Phys., 73, 4976, 1980.

This section will use gas-phase thermochemical data from Appendices 6 for molecules and 7 for radicals. These data include ionization energy (IE), electron affinity (EA), proton affinity (PA), gas-phase basicity (GB) and gas-phase acidity. Definitions of these parameters are given in Table 1.5. Some values of gas-phase basicities are given in Table 1.6.

Figure 1.48 displays experimental results of proton transfer under chemical ionization conditions. Exergonic reactions, that is $G° < 0$, are highly efficient, almost every collision giving rise to a proton transfer. However, the efficiency decreases sharply when the process becomes endergonic [107].

$G°$ values for some acids and bases can be found in the appendices to this book. Extensive values can be found in reference [108] or by internet at www.webbook.nist.gov.

1 ION SOURCES

As an example, let us examine whether or not the proton transfer from protonated ammonia to neutral aniline is efficient:

$$C_6H_5\text{-}NH_2 + NH_4^+ \longrightarrow C_6H_5\text{-}NH_3^+ + NH_3$$
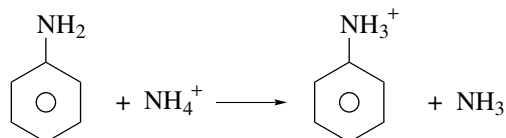
From the individual $\Delta G°$ values, equal to $-GB$, the $\Delta G°$ value for this reaction is calculated:

$$NH_4^+ \longrightarrow NH_3 + H^+ \qquad \Delta G° = -(-819)\ \text{kJ mol}^{-1}$$

$$C_6H_5\text{-}NH_2 + H^+ \longrightarrow C_6H_5\text{-}NH_3^+ \qquad \Delta G° = -851\ \text{kJ mol}^{-1}$$

_____

$$C_6H_5\text{-}NH_2 + NH_4^+ \longrightarrow C_6H_5\text{-}NH_3^+ + NH_3 \qquad \Delta G° = -32\ \text{kJ mol}^{-1}$$
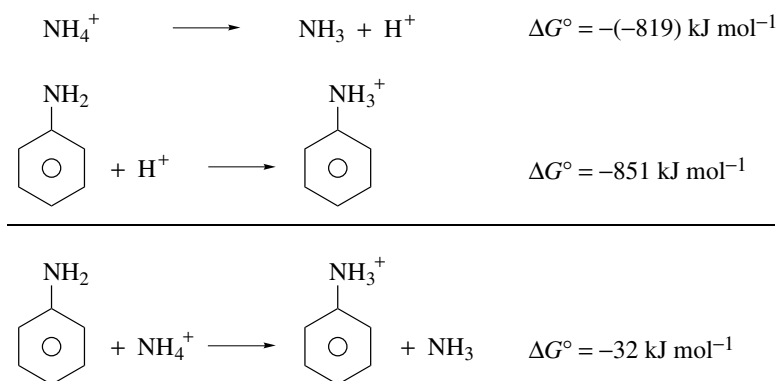
In a standard source, the reaction being exergonic, the proton transfer from ammonium to aniline will be very efficient. Note that in the source we are dealing here with efficiency at each collision, not with equilibrium. Under the high-vacuum conditions, equilibrium is not established. This example was selected because it shows that, in the gas phase, aniline is actually a stronger base than ammonia. The importance of solvation is thus emphasized once again. On the other hand, the methylamine is more basic than aniline:

$$CH_3\text{-}NH_2 + H^+ \longrightarrow CH_3\text{-}NH_3^+ \qquad \Delta G° = -864\ \text{kJ mol}^{-1}$$

$$C_6H_5\text{-}NH_3^+ \longrightarrow C_6H_5\text{-}NH_2 + H^+ \qquad \Delta G° = -(-851)\ \text{kJ mol}^{-1}$$

_____

$$C_6H_5\text{-}NH_3^+ + CH_3\text{-}NH_2 \longrightarrow C_6H_5\text{-}NH_2 + CH_3\text{-}NH_3^+ \qquad \Delta G° = -13\ \text{kJ mol}^{-1}$$
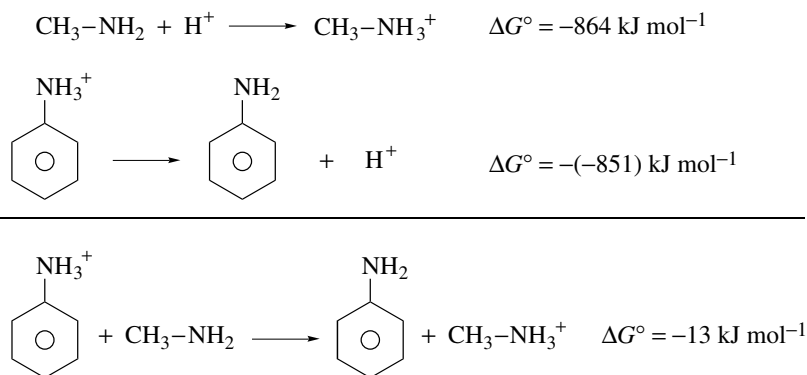
1.17 Formation and Fragmentation of Ions: Basic Rules

The aim of this section is to give an overview of the factors determining the formation of the various types of ions encountered in the different ionization modes. Exceptions

and examples are given in the sections dedicated to the ionization methods and to the fragmentations.

1.17.1 Electron Ionization and Photoionization Under Vacuum

These reactions occur under high vacuum. Thus, no ion–molecule reaction occurs. The species formed during the ionization process is a radical cation. Ionization efficiency depends on the ionization energy of the molecule. The presence or not of the molecular ions also depends on how easy it fragments.

Fragmentation often produces both a radical and a cation. This can be represented by the following equation:

$$R\text{–}R'^{\bullet +} \left\langle \begin{matrix} R^{\bullet} \ + \ R'^{+} \\ R^{+} \ + \ R'^{\bullet} \end{matrix} \right.$$
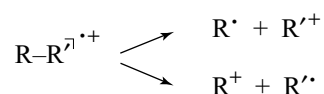
The factor that determines which of the fragments is a radical or a cation can be emphasized as a competition between two cations to capture the electron:

$$R^{+} \cdots e^{-} \cdots R'^{+}$$
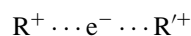
As the fragment with the higher propensity to retain the electron should have the higher ionization energy, the fragment observed in the spectrum as a cation is the one having the lowest ionization energy. The other one, having the highest ionization energy, takes the electron to be a radical. This is the origin of the Stevenson rule that will be explained in Chapter 7 on fragmentation.

1.17.2 Ionization at Low Pressure or at Atmospheric Pressure

The CI source operates at low pressure. Ion–molecule reactions occur and are needed for sample ionization. The MALDI source is under vacuum, but during the ionization process the pressure increases in the plume close to the target and ion–molecule reactions occur. The various sources operating at atmospheric pressure include ESI, APCI, APPI and AP-MALDI. All these sources operate at sufficient pressure to have numerous collisions between ions and molecules, and reactions between these species are observed.

It is worth noting that reactions between neutrals produced by fragmentations and ions are not observed. This is due to the fact that, whatever the ionization method, only a small fraction of the analyte molecules are ionized, and their fragments are at even lower concentrations. The probability of a collision is thus too low. Similarly, under normal conditions, no collision between ions is observed.

However, reactions may be observed between an ion and a neutral both resulting from the fragmentation of one precursor ion, immediately after cleavage, provided they remain associated for some time. This time is rarely more than a few microseconds. This can occur as well under vacuum as at higher pressure.

1.17.3 Proton Transfer

Proton transfer to produce a cation or an anion is the most often observed ion–molecule reaction in sources that allow collisions. The general rule is that the proton affinity of

the proton acceptor (neutral or anion) has to be higher than the proton affinity of the donor (cation or neutral). If there is a difference in proton affinity such that the reaction is exergonic, the transfer occurs at each collision (see Figure 1.48).

The protonated molecule fragments, if necessary after activation. The fragments do not always result from the cleavage of only one bond, as this can lead to the formation of a radical fragment and a radical cation, a very unfavorable process. The pathway is thus often more complicated than for radical cations. It can be represented as follows:

$$M + H^+ \longrightarrow MH^+$$

$$MH^+ \begin{array}{c} \nearrow Fl + F2H^+ \\ \searrow FlH^+ + F2 \end{array}$$

$$Fl \cdots H^+ \cdots F2$$
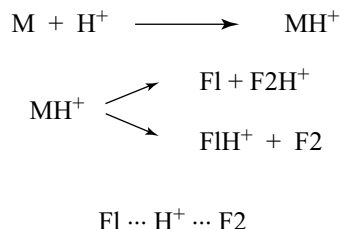
Here the competition is between two fragments for a proton. The fragment with the highest gas-phase basicity gets the proton. For negative ions a similar rule applies, but now it is the most acidic species that carries the negative charge. This is analogous to the competition seen before, about EI, between two ions for an electron.

A similar competition already exists at the ion formation stage in the source. For this reason, in the presence of a solvent having a certain proton affinity, it is not possible to see the protonated cation of an analyte having a lower proton affinity. It is, however, possible to observe an adduct with another cation, such as sodium, ammonium, and so on. The reverse is true for negative ions. Here too, adducts with anions as chloride, acetate, and so on may be observed.

Similarly, if two analytes in a mixture have a marked difference of acidity or basicity, only one is observed in the spectrum: the best proton acceptor in positive ion mode, or the best proton donor in negative ion mode. However, at low concentrations the competition is less obvious, and both ions can sometimes be observed together.

1.17.4 Adduct Formation

An adduct is an ion formed by direct combination of a neutral molecule and an 'ionizing' ion other than the proton. In positive ion mode the most often observed is the sodium adduct, producing an ion with 22 mass units higher than the protonated molecule, that is $(M + 23)^+$ instead of $(M + 1)^+$. It is often accompanied by a potassium adduct, another 16 u higher:

$$M + Na^+ \longrightarrow (M + Na)^+$$
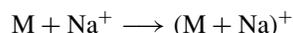
Extended tables of gas-phase proton affinity exist. This is not true for the affinity towards metal ions. To attach a proton a basic site is needed. Binding a sodium ion requires the availability of several electron pairs in its surrounding. Sugars for example are not basic, but a sodium ion may find many electron pairs. This is why the protonated molecule is difficult to observe in the mass spectrum if the solution is not carefully desalted. Otherwise,

the sodium adduct is dominant. If ammonium salt is present it can also form adducts $(M + NH_4)^+$ because of its ability to form hydrogen bonds.

In the negative ion mode, the chloride adduct is often observed yielding $(M + 35)^-$ and $(M + 37)^-$. As for the sodium, the chloride ion is always present if the solution is not desalted. However, it produces fewer adducts than the sodium. The acetate ions, if present, produce $(M + 59)^-$ owing to their ability to form hydrogen bonds.

The addition of ammonium acetate, at low concentration, in API methods can be interesting to produce protonated or deprotonated species. Indeed, in the heated gas or heated capillary interface, ammonia or acetic acid evaporates, leaving the corresponding protonated or deprotonated species. The interest of nitrate adducts in the analysis of sugars has been recently demonstrated [109, 110].

1.17.5 Formation of Aggregates or Clusters

'Dimer' ions such as $(M + M + H)^+$ or of higher order $(nM + H)^+$ are often observed. The proton can be replaced by another cation. 'Heterodimers' of the general formula $(M + M' + H)^+$, or with a metal cation or of higher order, are also observed. The corresponding ions are also observed in negative ion mode.

It should be noted that the formation of such aggregates in the gas phase causes a diminution of entropy. To be possible, the formation of such aggregates must be exothermic. Furthermore, if the partners have similar basicities or affinities for the cation, the cluster is more stable. Otherwise it dissociates, one of the partners taking the proton, or the cation, according to the relative stability. This is why associations of two or more identical molecules are observed more often or at higher abundances. Indeed, they have the same affinities of course.

The formation of oligomers has as a consequence the diminution of the number of molecules in the gas phase, and thus occurs with a diminution of the entropy. As the reaction must be exergonic to occur, it must be sufficiently exothermic, at least to compensate for the entropy loss. Once formed, the internal energy of the oligomer should be reduced, since it contains a sufficient amount of energy to dissociate. This needs a collision with a third partner, and this requires a sufficient pressure.

As a general rule, the abundance is reduced when the number of associated molecules increases. However, some specific aggregates, resulting from particularly important interactions, are present at particularly high abundance. This occurs often with organometallic compounds, as the metal tries to complete its electronic shell.

Aggregates are rarely observed in the negative ion mode, because the presence of the negative charge causes an expansion of the electronic shell, thus reducing the electric field around the negatively charged ion. This reduces the interactions between the partners.

1.17.6 Reactions at the Interface Between Source and Analyser

Atmospheric pressure sources need to have a device for the desolvation of the ions, such as a heated capillary, a heated gas curtain, collisions at intermediate pressure in a focusing multipole. The increase in internal energy induces the dissociation of the associated ion–molecules. Furthermore, the ions are at low pressure and thus the probability of the reverse reaction is strongly decreased. For example, if a molecule forms a complex with an

ammonium ion, the ammonia can be evacuated by pumping:

$$(M + NH_4)^+ \longrightarrow (M + H)^+ + NH_3$$
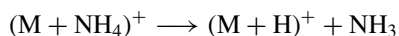
This reaction occurs even if M is less basic than ammonia. So, the protonated molecular ion of a sugar may be formed by desolvatation of its ammoniacal complex.

In negative ion mode, the acetate ion is used and acetic acid can be evacuated by pumping to obtain the deprotonated molecular ion of the analyte:

$$(M + AcO)^- \longrightarrow (M - H)^- + AcOH$$
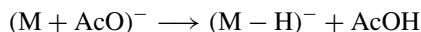
References

1. Bleakney, W. (1929) *Phys. Rev.*, **34**, 157.
2. Nier, A.O. (1947) *Rev. Sci. Instrum.*, **18**, 415.
3. Bentley, T.W. and Johnstone, R.A.W. (1970) Mechanism and structure in mass spectrometry: a comparison with other chemical processes, in *Advances in Physical Organic Chemistry*, vol. **8** (ed. V. Gold), Academic Press, London.
4. Kienitz, H. (1968) *Massenspektrometrie*, Verlag Chemie, Weinheim, p. 45.
5. Harrison, A.G. (1983) *Chemical Ionisation Mass Spectrometry*, CRC Press, Boca Raton, FL.
6. Thermodynamic data from: Lias, S.G., Bartmess, J.E., Liebman, J.F. *et al.* (1988) Gas-phase ion and neutral thermochemistry. *J. Phys. Chem. Ref. Data*, **17** (Suppl. 1). Also available on laser disk from NIST (National Institute of Standards and Technology), Washington, DC, USA).
7. Baldwin, M.A. and McLafferty, F.W. (1973) *Org. Mass Spectrom.*, **7**, 1353.
8. Beckey, H.D. (1969) Field ionization mass spectrometry. *Research/Development*, **20**, 26–9.
9. Van Vaeck, L., Adriaens, A. and Gijbels, R. (1999) Static secondary ion mass spectrometry: (S-SIMIS) Part 1. Methodology and structural information. *Mass Spectrom. Rev.*, **18** (1), 1–47.
10. Adriaens, A., Van Vaeck, L. and Adams, F. (1999) Static secondary ion mass spectrometry: (S-SIMIS) Part 2. Material sciences applications. *Mass Spectrom. Rev.*, **18** (1), 48–81.
11. Benninghoven, A. and Sichtermann, W.K. (1978) *Anal. Chem.*, **50**, 1180.
12. Barber, M., Bardoli, R.S., Sedgwick, R.D. and Tyler, A.H. (1981) *J. Chem. Soc., Chem. Commun.*, 325.
13. Aberth, W., Straub, K.M. and Burlingame, A.L. (1982) *Anal. Chem.*, **54**, 2029.
14. Beckey, H.D. (1977) *Principles of Field Ionization and Field Desorption in Mass Spectrometry*, Pergamon Press, Oxford.
15. Mcfarlane, R.D. and Torgesson, T.F. (1976) *Science*, **191**, 970.
16. McNeal, C.J. and McFarlane, R.D. (1981) *J. Am. Chem. Soc.*, **103**, 1609.
17. Karas, M. and Hillenkamp, F.H. (1988) *Anal. Chem.*, **60**, 2229.
18. Hillenkamp, F., Karas, M., Ingeldoh, A. and Stahl, B. (1990) Matrix assisted UV-laser desorption ionization: a new approach to mass spectrometry of large molecules, in *Biological Mass Spectrometry*, p. 49 (eds A.L. Burlingame and J.A. McCloskey), Elsevier, Amsterdam.
19. Karas, M., Bachmann, D., Bahr, U. and Hillenkamp, F. (1987) *Int. J. Mass Spectrom. Ion Processes*, **78**, 53.
20. Karas, M. and Hillenkamp, F.H. (1988) *Anal. Chem.*, **60**, 2229.

21. Hillenkamp, F., Karas, M., Ingeldoh, A. and Stahl, B. (1990) Matrix assisted UV-laser desorption ionization: a new approach to mass spectrometry of large molecules, in *Biological Mass Spectrometry* (eds A.L. Burlingame and J.A. McCloskey), Elsevier, Amsterdam, p. 49.
22. Stump, M.J., Fleming, R.C., Gong, W.-H. *et al.* (2002) *Appl. Spectrosc. Rev.*, **37**, 275.
23. Chen, X.J., Carroll, J.A. and Beavis, R.C. (1998) Near-UV-induced matrix-assisted laser desorption/ionization as a function of wavelength. *J. Am. Soc. Mass Spectrom.*, **9** (9), 885−91.
24. Knochenmuss, R. (2002) A quantitative model of UV matrix-assisted laser desorption/ ionization. *J. Mass Spectrom.*, **37**, 867.
25. Karas, M. and Kruger, R. (2003) *Chem. Rev.*, **103**, 427.
26. Dreisewerd, K. (2003) *Chem. Rev.*, **103**, 395.
27. Zenobi, R. and Knochenmuss, R. (1998) Ion formation in MALDI mass spectrometry. *Mass Spectrom. Rev.*, **17** (5), 337–66.
28. Knochenmuss, R. and Zenobi, R. (2003) *Chem. Rev.*, **103**, 441.
29. Karas, M. and Hillenkamp, F.H. (1988) *Ion Formation from Organic Solids IV* (ed. A. Benninghoven), John Wiley & Sons, Inc., New York, p. 103.
30. Spengler, B. and Cotter, R.J. (1990) *Anal. Chem.*, **62**, 793.
31. Pasch, H. and Schrepp, W. (2003) *MALDI-TOF Mass Spectrometry of Synthetic Polymers*, Series: Springer Laboratory XVIII.
32. Hillenkamp, F.H. and Karas, M. (1990) *Methods in Enzymology*, vol. **193** (ed. J.A. McCloskey), Academic Press, New York, pp. 280–95.
33. Stoeckli, M., Chaurand, P., Hallahan, D.E. and Caprioli, R.M. (2001) *Nat. Med.*, **7**, 493.
34. Pierson, J., Norris, J.L., Aerni, H.R. *et al.* (2004) *J. Proteome Res.*, **3**, 289.
35. Demirev, P., Westman, A., Reimann, C.T. *et al.* (1992) *Rapid Commun. Mass Spectrom.*, **6**, 187.
36. Talrose, V. L., Person, M.D., Whittal, R.M. *et al.* (1999) *Rapid Commun. Mass Spectrom.*, **13**, 2191.
37. Vorm, O., Roepstorff, P. and Mann, M. (1994) *Anal. Chem.*, **66**, 3281.
38. Xiang, F. and Beavis, R.C. (1994) *Rapid Commun. Mass Spectrom.*, **8**, 199.
39. http://www.chemistry.wustl.edu/˜msf/damon/sample_prep_toc.html" (21 March 2007).
40. http://www.nist.gov/maldi (21 March 2007).
41. Vorm, O., Chait, B.T. and Roepstorff, P. (1994) *Mass Spectrometry of Protein Samples Containing Detergents*, 41th ASMS Conference Proceedings, pp. 621a–b.
42. Merchant, M. and Weinberger, S.R. (2000) *Electrophoresis*, **21**, 1164.
43. Chen, Y.C., Shiea, J. and Sunner, J. (1998) *J. Chromatogr. A*, **826**, 77.
44. Shen, Z.X., Thomas, J.J., Averbuj, C. *et al.* (2001) *Anal. Chem.*, **73**, 612.
45. Laiko, V.V., Baldwin, M.A. and Burlingame, A.L. (2000) *Anal. Chem.*, **72**, 652–7.
46. Laiko, V.V., Moyer, S.C. and Cotter, R.J. (2000) *Anal. Chem.*, **72**, 5239–43.
47. Moyer, S.C. and Cotter, R.J. (2002) *Anal. Chem.*, **74**, 469A.
48. Vestal, M.L. (1983) *Mass Spectrom. Rev.*, **2**, 447.
49. Blakney, C.R. and Vestal, M.L. (1983) *Anal. Chem.*, **55**, 750.
50. Huang, E.C., Wachs, T., Conboy, J.J. and Henion, J.D. (1990) *Anal. Chem.*, **62**, 713A.
51. Bruins, A.P. (1991) *Mass Spectrom. Rev.*, **10**, 53.
52. Mann, M., Meng, C.K. and Fenn, J.B. (1989) Interpreting mass spectra of multiply charged ions. *Anal. Chem.*, **61**, 1702–8.
53. Fenn, J.B., Mann, M., Meng, C.K. *et al.* (1989) *Science*, **246**, 64.
54. de la Mora, J.F., Van Berkel, G.J., Enke, C.G. *et al.* (2000) Electrochemical processes in electrospray ionization mass spectrometry. *J. Mass. Spectrom.*, **35**, 939–52.

55. Cech, N.B. and Enke, C.G. (2001) Practical implications of some recent studies in electrospray ionization fundamentals. *Mass Spectrom. Rev.*, **20**, 362–87.

56. Rohner, T.C., Lion, N. and Girault, H.H. (2004) Electrochemical and theoretical aspects of electrospray ionisation. *Phys. Chem. Chem. Phys.*, **6**, 3056–68.

57. Snyder, A.P. (ed.) (1996) *Biochemical and Biotechnological Applications of Electrospray Ionization Mass Spectrometry*, ACS Symposium Series 619, American Chemical Society, Washington, DC.

58. Cole, R.B. (ed.) (1997) *Electrospray Ionisation Mass Spectrometry*, John Wiley & Sons, Ltd., Chichester.

59. Yamashita, M. and Fenn, J.B. (1988) *Phys. Chem.*, **88**, 4451.

60. Yamashita, M. and Fenn, J.B. (1988) *Phys. Chem.*, **88**, 4671.

61. Loo, J.A., Udseth, H.R. and Smith, R.D. (1989) *Anal. Biochem.*, **179**, 404.

62. Ikonomou, M.G., Blades, A.T. and Kebarle, P. (1990) *Anal. Chem.*, **62**, 957.

63. Smith, R.D., Loo, J.A., Edmons, C.G. *et al.* (1990) *Anal. Chem.*, **62**, 882.

64. Mann, M. (1990) *Org. Mass Spectrom.*, **25**, 575.

65. Kebarle, P. and Tang, L. (1993) From ions in solution to ions in the gas phase. The mechanism of electrospray mass spectrometry. *Anal. Chem.*, **65**, 972A.

66. Gomez, A. and Tang, K. (1994) *Phys. Fluids*, **6**, 404.

67. Andersen, J., Molina, H., Moertz, E. *et al.* (1998) Quadrupole-TOF hybrid mass spectrometers bring improvements to protein identification and MS/MS analysis of intact proteins. *The 46th Conference on Mass Spectrometry and Allied Topics*, Orlando, Florida, p. 978.

68. van Berkel, W.J.H., van den Heuvel, R.H.H., Versluis, C. and Heck, A.J.R. (2000) Detection of intact megaDalton protein assemblies of vanillyl-alcohol oxidase by mass spectrometry. *Protein Sci.*, **9**, 435–9.

69. Kelly, M.A., Vestling, M.M., Fenselau, C. and Smith, P.B. (1992) *Org. Mass Spectrom.*, **27**, 1143.

70. Covey, T. (1996) Analytical characteristics of the electrospray ionization process, in *Biochemical and Biotechnological Applications of Electrospray Ionization Mass Spectrometry*, pp. 21–59 (ed. A.P. Snyder), ACS Symposium Series 619, American Chemical Society, Washington, DC.

71. Emmett, M.R. and Caprioli, R.M. (1994) *J. Am. Soc. Mass Spectrom.*, **5**, 605.

72. Wilm, M. and Mann, M. (1994) *Proceedings of the 42nd ASMS Conference*, Chicago, p. 770.

73. Wilm, M., Shevchenko, A., Houthaeve, T. *et al.* (1996) Femtomole sequencing of proteins from polyacrylamide gels by nano-electrospray mass spectrometry. *Nature*, **379** (6564), 466–9.

74. Van Berkel, G.J. and Zhou, F. (1995) *Anal. Chem.*, **67**, 2916.

75. Fenn, J.B., Rosell, J., Nohmi, T. *et al.* (1996) Electrospray ion formation: desorption versus desertion, in *Biochemical and Biotechnological Applications of Electrospray Ionization Mass Spectrometry*, pp. 60–80 (ed. A.P. Snyder), ACS Symposium Series 619, American Chemical Society, Washington, DC.

76. Carroll, D.I., Dzidic, I., Stillwell, R.N. *et al.* (1975) *Anal. Chem.*, **47**, 2369.

77. French, J.B. and Reid, N.M. (1980) *Dynamic Mass Spectrometry*, vol. **6**, Heyden, London, pp. 220–33.

78. Bruins, A.P. (1991) *Mass Spectrom. Rev.*, **10**, 53.

79. Cambier, V., Hance, T. and de Hoffmann, E. (1999) Non-injured maize contains several 1,4-benzoxazin-3-one related compounds but only as glucoconjugates. *Phytochem. Anal.*, **10**, 119–26.

80. Robb, D.B., Covey, T.R. and Bruins, A.P. (2000) *Anal. Chem.*, **72**, 3653.

81. Syage, J.A. and Evans, M.D. (2001) *Spectroscopy*, **16**, 14.
82. Kauppila, T.J., Kuuranne, T., Meurer, E.C. *et al.* (2002) *Anal. Chem.*, **74**, 5470.
83. Syage, J.A. (2004) *J. Am. Soc. Mass Spectrom.*, **15**, 1521.
84. Kauppila, T.J., Kotiaho, T., Kostiainen, R. and Bruins, A.P. (2004) *J. Am. Soc. Mass Spectrom.*, **15**, 203.
85. Raffaelli, A. and Saba, A. (2003) *Mass Spectrom. Rev.*, **22**, 318.
86. Takats, Z., Wiseman, J.M., Gologan, B. and Cooks, R.G. (2004) Mass spectrometry sampling under ambient conditions with electrospray ionization. *Science*, **306**, 471–3.
87. Kertezs, V., Ford, M.J. and Van Berkel, G.J. (2005) Automation of a surface sampling probe/electrospray mass spectrometry system. *Anal. Chem.*, **77**, 7183–9.
88. Cody, R.B., Laramee, J.A. and Dupont Durst, H. (2005) Versatile new ion source for the analysis of materials in open air under ambient conditions. *Anal. Chem.*, **77**, 2297–302.
89. Adams, F., Gijbels, R. and Van Grieken, R. (1988) *Inorganic Mass Spectrometry (Chemical Analysis: A Series of Monographs on Analytical Chemistry and Its Applications)*, vol. 95, John Wiley & Sons, Inc., New York.
90. Gijbels, R., Van Straaten, M. and Bogaerts, A. (1995) *Adv. Mass Spectrom.*, **13**, 241−56.
91. Becker, J.S. and Dietze, H.J. (1998) Inorganic trace analysis by mass spectrometry. *Spectrochim. Acta Part B – At. Spectrosc.*, **53** (11), 1475–1506.
92. Steward, I.I. and Horlick, G. (1996) Developments in the electrospray mass spectrometry of inorganic species. *Trends Anal. Chem.*, **15** (2), 80–90.
93. Traeger, J.C. and Colton, R. (1998) *Adv. Mass Spectrom.*, **14**, 637–659.
94. Colton, R., D'Agostino, A. and Traeger, J.C. (1999) Electrospray mass spectrometry applied to inorganic and organometallic chemistry. *Mass Spectrom. Rev.*, **14** (2), 79–106.
95. Inghram, M.G. and Chupka, W.A. (1953) *Rev. Sci. Instrum.* **24**, 518.
96. Heumann, K.G., Eisenhut, S., Gallus, S. *et al.* (1995) *Analyst*, **120** (5), 1291–9.
97. Johnson, P.G., Bolson, A. and Henderson, C.M. (1973) *Nucl. Instrum. Methods*, **106**, 83.
98. Dempster, A.J. (1936) *Rev. Sci. Instrum.*, **7**, 46.
99. Harrison, W.W. and Hang, W. (1996) Powering the analytical glow discharge. *Fresenius J. Anal. Chem.*, **355** (7–8), 803–7.
100. Bogaerts, A. and Gijbels, R. (1998) Fundamental aspects and applications of glow discharge spectrometric techniques. *Spectrochim. Acta Part B – At. Spectrosc.*, **53** (1), 1–42.
101. Hang, W., Yan, X.M., Wayne, D.M. *et al.* (1999) Glow discharge source interfacing to mass analyzers: Theoretical and practical considerations. *Anal. Chem.*, **71** (15), 3231–7.
102. Gray, A.L. (1985) *Spectrochim. Acta Part B – At. Spectrosc.*, **40**, 1525.
103. Zoorob, G.K., McKiernan, J.W. and Caruso, J.A. (1998) ICP-MS for elemental speciation studies. *Mikrochim. Acta*, **128** (3–4), 145–68.
104. Hill, S.J. (1999) *ICP Spectrometry and its Applications*, Sheffield Academic Press, Sheffield, p. 320.
105. McIver, R.T. (1980) *Sci. Am.*, **243**, 148.
106. Bohme, D.K. and Mackay, G.I. (1981) *J. Am. Chem. Soc.*, **103**, 978.
107. Bohme, D., Mackay, G.I. and Schiff, H.I. (1980) *J. Chem. Phys.*, **73**, 4976.
108. Lias, S.G., Bartmess, J.E., Liebman, J.F. *et al.* (1988) Gas-phase ion and neutral thermochemistry. *J. Phys. Chem. Ref. Data*, **17** (Suppl. 1).
109. Jiang, Y. and Cole, R.B. (2005) Oligosaccharide analysis using anion attachment in negative mode electrospray mass spectrometry. *J. Am. Soc. Mass Spectrom.*, **16** (1), 60–70.
110. Harvey, D.J. (2005) Fragmentation of negative ions from carbohydrates: Part 1. Use of nitrate and other anionic adducts for the production of negative ion electrospray spectra from N-linked carbohydrates. *J. Am. Soc. Mass Spectrom.*, **16** (5), 622–30.